The Stirring Tropics: Theory of Moisture Mode–Hadley Cell Interactions

Ángel F. Adames Corraliza, Víctor C. Mayta

Department of Atmospheric and Oceanic Sciences, University of Wisconsin, Madison, Wisconsin

Corresponding author: Ángel F. Adames Corraliza, angel.adamescorraliza@wisc.edu

Early Online Release: This preliminary version has been accepted for publication in *Journal of Climate*, may be fully cited, and has been assigned DOI 10.1175/JCLI-D-23-0147.1. The final typeset copyedited article will replace the EOR at the above DOI when it is published.

ABSTRACT: Interactions between large-scale waves and the Hadley Cell are examined using a linear two-layer model on an f-plane. A linear meridional moisture gradient determines the strength of the idealized Hadley Cell. The trade winds are in thermal wind balance with a weak temperature gradient (WTG). The mean meridional moisture gradient is unstable to synoptic-scale (horizontal scale of ∼1000 km) moisture modes that are advected westward by the trade winds, reminiscent of oceanic tropical depression-like waves. Meridional moisture advection causes the moisture modes to grow from "moisture-vortex instability" (MVI), resulting in a poleward eddy moisture flux that flattens the zonal-mean meridional moisture gradient, thereby weakening the Hadley Cell. The amplification of waves at the expense of the zonal-mean meridional moisture gradient implies a downscale latent energy cascade. The eddy moisture flux is opposed by a regeneration of the meridional moisture gradient by the Hadley Cell. These Hadley Cell-moisture mode interactions are reminiscent of quasi-geostrophic interactions, except that wave activity is due to column moisture variance rather than potential vorticity variance. The interactions can result in predator-prey cycles in moisture mode activity and Hadley Cell strength that are akin to ITCZ breakdown. It is proposed that moisture modes are the tropical analog to midlatitude baroclinic waves. MVI is analogous to baroclinic instability, stirring latent energy in the same way that dry baroclinic eddies stir sensible heat. These results indicate that moisture modes stabilize the Hadley Cell, and may be as important as the latter in global energy transport.

Accepted for publication in *Journal of Climate*. DOI 10.1175/JCLI-D-23-0147.1.

SIGNIFICANCE STATEMENT: The tropics are characterized by steady circulations such as the Hadley Cell as well as a menagerie of tropical weather systems. Despite progress in our understanding of both, little is known about how the mean circulations and the weather systems interact with one another. Here we show that tropical waves can grow by extracting moisture from the Hadley Cell, thereby weakening it. They also transport moisture to higher latitudes. Our results challenge the notion that the Hadley Cell is the sole transporter of energy out of the tropics and instead favor a view where tropical waves are also essential for the global energy balance. They dry the humid regions and moisten the drier regions via stirring.

1. Introduction

Prior to the second world war, many atmospheric scientists believed the tropics to be very stable outside of the occasional occurrence of tropical cyclones (see prologue in Riehl 1954). As interest in the tropics grew and observations increased, scientists showed that the tropics contain a diversity of "tropical weather systems" that exhibit a wide variety of spatial and temporal scales. Near the equator, studies have documented the existence of convectively-coupled equatorial waves (Matsuno 1966; Kiladis et al. 2009), and the Madden-Julian Oscillation (Madden and Julian 1972). Away from the equator, we see tropical cyclones and a variety of tropical depression-like (TD-like) systems that include monsoon low-pressure systems and easterly waves (Riehl 1954; Chang 1970; Mooley 1973)

Interestingly, such a diversity of systems exists within an atmosphere that exhibits little spatial and temporal variations in temperature (Charney 1963; Held and Hoskins 1985), leading to the development of the weak temperature gradient (WTG) approximation (Sobel and Bretherton 2000; Sobel et al. 2001). They also coexist with the mean circulations: the Hadley and Walker Cells, and the monsoons. These large-scale systems are known to export energy from the source regions to net sink regions (Riehl and Malkus 1958; Held and Hou 1980; Hartmann 2015).

Analysis of the governing thermodynamics of these systems has indicated that tropical weather systems exist in a spectrum (Adames et al. 2019; Inoue et al. 2020; Adames and Maloney 2021; Mayta and Adames 2023). Systems that propagate quickly exhibit thermodynamics that are governed by temperature fluctuations, as in gravity waves (Raymond et al. 2007; Herman et al. 2016). These are the systems that are responsible for maintaining WTG balance over the tropics

Accepted for publication in *Journal of Climate*. DOI 10.1175/JCLI-D-23-0147.1.

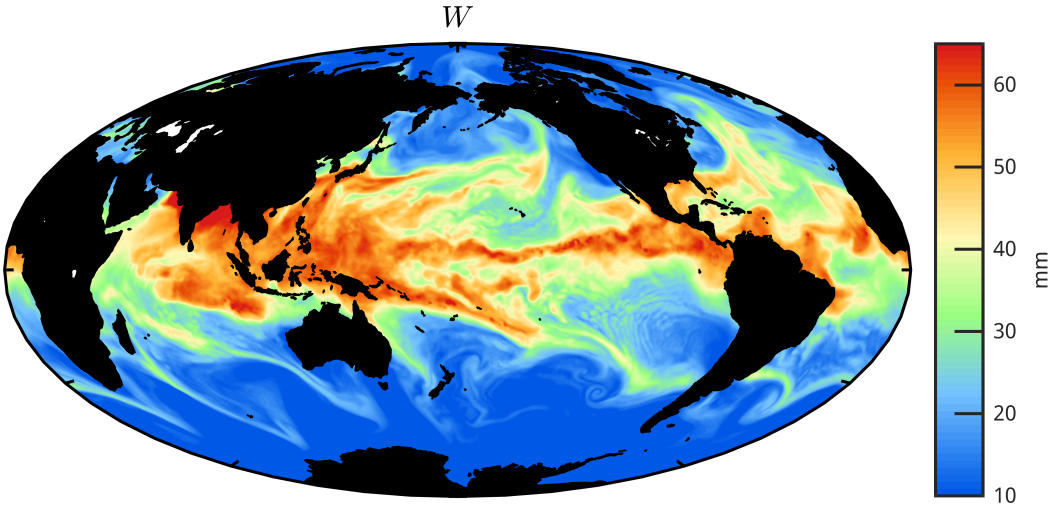

FIG. 1. Snapshot of ERA5 column-integrated water vapor (W) for June 29, 2017. Lands are masked out to emphasize the wavy behavior over the oceans.

(Bretherton and Smolarkiewicz 1989; Wolding et al. 2016). Slower-evolving convectively-coupled systems are often in WTG balance and their thermodynamics are governed by moisture, hence the moniker "moisture modes" (Yu and Neelin 1994; Raymond and Fuchs 2009; Adames and Maloney 2021).

Initially, only the MJO was hypothesized to be a moisture mode (Raymond and Fuchs 2009; Sugiyama 2009; Sobel and Maloney 2013). Numerous advances in our understanding of the MJO have resulted from its study under the moisture mode lens (see reviews by Zhang et al. 2020, Jiang et al. 2020 and Adames et al. 2021). While the idea of the MJO being a moisture mode remains a topic of debate (Powell 2017; Chen 2022a; Mayta and Adames Corraliza 2023a), other studies have indicated that moisture modes may be a broader feature of the tropics (Adames 2022; Inoue et al. 2020; Maithel and Back 2022; Mayta and Adames 2023). On the basis of scale analysis, Adames et al. (2019) and Adames (2022) showed that systems with propagation speeds near 5 m s^{-1} are likely to be moisture modes. Such systems include most "rotational" tropical systems such as convectively-coupled equatorial Rossby waves and TD-like systems.

Over the western hemisphere, observations indicate equatorial Rossby waves and oceanic TD-like waves are moisture modes (Mayta et al. 2022; Mayta and Adames 2023). The same results were identified over the eastern and western Pacific and over the Indian Ocean (Gonzalez and

Accepted for publication in *Journal of Climate*. DOI 10.1175/JCLI-D-23-0147.1.

Jiang 2019; Nakamura and Takayabu 2022a,b; Chen 2022b; Mayta and Adames Corraliza 2023b). Only African easterly waves do not fully exhibit moisture mode properties (Wolding et al. 2020; Núñez Ocasio and Rios-Berrios 2023; Vargas Martes et al. 2023). Wavenumber-frequency analysis also supports this hypothesis (Inoue et al. 2020). Storm-permitting simulations on an aquaplanet also reveal a high variance of moisture mode-like behavior in the form of easterly wave-like disturbances (Rios-Berrios et al. 2023). More recently, Maithel and Back (2022) found that convective recharge-discharge cycles can be explained well if these are assumed to behave like moisture modes. All these results allude to the potential commonality of moisture modes.

In spite of their geographical and structural differences, all these moisture modes are driven by the same processes. Their moist static energy (MSE) anomalies are governed by moisture and they propagate westward via horizontal moisture advection (Yasunaga et al. 2019; Inoue et al. 2020; Mayta and Adames Corraliza 2023b). Many studies have shown that vertical MSE advection dissipates the systems while longwave radiative supports their growth (Andersen and Kuang 2012; Sobel et al. 2014; Mayta et al. 2022). A less documented feature of these systems is that the advection of background-mean MSE by the anomalous meridional winds also contributes to their growth (Mayta and Adames Corraliza 2023b). This type of growth was initially documented in the balanced moisture waves of Sobel et al. (2001) and was later coined by Adames and Ming (2018) as "moisture-vortex instability". While this instability was initially posited to explain the growth of monsoon low-pressure systems (Adames and Ming 2018), a companion study (Mayta and Adames Corraliza 2023b)(MA henceforth) suggests that this mechanism is present in TD-like waves and equatorial Rossby waves around the globe. Most of these systems also have the common feature that they are advected westward by the mean winds (Russell et al. 2020; Gonzalez and Jiang 2019, MA).

We hypothesize that the self-similarity of these balanced waves may be a fundamental feature of their interaction with the tropical mean state. This hypothesis is further strengthened by examining a snapshot of column-integrated water vapor for a typical day of tropical wave activity (Fig. 1). In it, we see that the humid regions of the tropics appear wavy, even when there is no obvious sign of extratropical forcing. This large-scale behavior hints at the possibility that tropical waves may actively "stir" column water vapor, mixing it throughout the tropics.

Accepted for publication in *Journal of Climate*. DOI 10.1175/JCLI-D-23-0147.1.

Observational support for this hypothesis already exists. Sherwood (1996) and Pierrehumbert (1998) showed that the subtropics can be moistened by horizontal transports of water vapor from the convecting regions. Conversely, many studies have shown that tongues of dry subtropical air can intrude into the rainy regions of the tropics, suppressing rainfall (Mapes and Zuidema 1996; Parsons et al. 2000; Jensen and Del Genio 2006; Kerns and Chen 2014). Inoue et al. (2021) found that horizontal moisture advection is the primary cause of precipitation variability in the tropics. Furthermore, analysis of the poleward energy transport in the tropics shows a non-negligible poleward latent energy transport by transients at the sub-monthly timescale (Trenberth and Stepaniak 2003; Peters et al. 2008; Rios-Berrios et al. 2020), suggesting that this stirring is also important for the global energy balance. These eddy moisture transports have been found to behave as a moisture diffusion (Sobel and Neelin 2006; Peters et al. 2008), weakening the ITCZ and moistening the midlatitudes. MA showed that a statistically-significant signal in poleward moisture transport exists in all the westward-propagating moisture modes they examined.

The similarity of moisture modes across the tropics becomes more intriguing when we compare them to unstable baroclinic waves. One of the main features of dry baroclinic instability is that they grow from meridional temperature advection. The phasing between meridional winds and the temperature anomalies causes the growing waves to exhibit a poleward heat flux, a major piece of midlatitude wave-mean flow interactions as crystalized in the Eliassen-Palm formulation of wave activity (Andrews and Mcintyre 1976; Edmon Jr et al. 1980). The heat flux acts to weaken the horizontal temperature gradient, therefore weakening the jet stream via thermal wind balance. If not for these fluxes, the temperature difference between the tropics and the globe would be larger than observed.

This study aims to examine the possibility that an analogous wave-mean flow interaction exists in the tropics. In this analogy the moisture modes are akin to the baroclinic waves, interacting with the mean state via moisture advection rather than temperature advection. The Hadley Cell is the analog of the midlatitude jet stream. As in baroclinic instability, we hypothesize that *moisture modes grow by extracting energy from the mean meridional moisture gradient (i.e., MVI), flattening it and therefore weakening the Hadley Cell.*

In order to test this hypothesis, we will employ a simple two-layer model to examine how an idealized circulation could lead to the existence of moisture modes (Section 2). Then, we

Accepted for publication in *Journal of Climate*. DOI 10.1175/JCLI-D-23-0147.1.

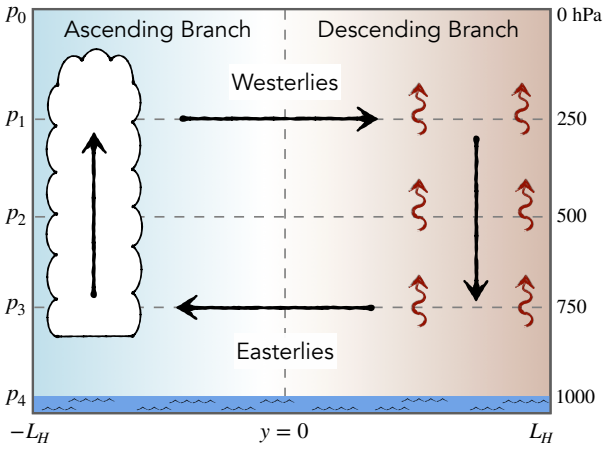

FIG. 2. Schematic describing the two-layer moist model on an f-plane used in this study. The arrows depict the direction of the overturning circulation. Blue shading indicates the humid ascending and brown indicates the dry, subsiding branch. Pressure levels in the model are shown on the left and their values are shown on the right. The cloud indicates the region of convective heating and the curly arrows indicate the radiative cooling.

will examine the properties of these waves, including their propagation and growth (Section 3). Interactions between moisture modes and the Hadley Cell are discussed in Section 4. A concluding discussion about the main findings of this study is offered in Section 5.

2. Two-layer model

a. Model setup

We are particularly interested in capturing the moisture mode behavior of oceanic TD-like waves and how these may interact with an idealized Hadley Cell. Studies using observations and reanalysis show that these waves exhibit little tilt in height in their vertical velocity field (Serra et al. 2008; Inoue et al. 2020; Feng et al. 2020a,b; Huaman et al. 2021). This lack of tilting implies that the two-layer model with a simplified profile of vertical velocity used by Adames (2021) (A21 henceforth) may adequately capture their behavior. This is the same model shown in Holton and Hakim (2012) except modified to include a prognostic moisture budget. This model allows us to include the effects of vertical wind shear but is also sufficiently simple to allow for a tractable analysis of its wave solutions. The main variables in this study are outlined in Table 1 and constants with their values are shown in Table 2.

Accepted for publication in *Journal of Climate*. DOI 10.1175/JCLI-D-23-0147.1.

TABLE 1. The main variables and definitions used in this study.

Var.	*Description*	*Units*
ψ	Streamfuction	$m^2\ s^{-1}$
Ψ	Mass streamfuction	$kg\ s^{-1}$
Φ	Geopotential	$m^2\ s^{-2}$
T	Temperature	K
$\mathbf{v}$	Horizontal wind vector	$m\ s^{-1}$
ω	Vertical pressure velocity	$Pa\ s^{-1}$
ζ	Relative vorticity	s^{-1}
δ	Horizontal divergence	s^{-1}
$L_v P$	Surface precipitation rate	$W\ m^{-2}$
$L_v E$	Surface latent heat flux	$W\ m^{-2}$
C	Column processes	$kg\ m^{-2}\ s^{-1}$
R_{cs}	Clear-sky radiative cooling rate	$W\ m^{-2}$
r	Cloud-radiative feedback parameter	-
q	Specific humidity	$kg\ kg^{-1}$
W	Column-integrated moisture	$kg\ m^{-2}$
S	Gross dry stability	$J\ m^{-2}$
τ_c	Conv. moisture adjustment timescale	s
β_q	Mean meridional moisture gradient	$m^{-1}\ s^{-1}$
ϖ	Wave frequency	s^{-1}
k	Zonal wavenumber	m^{-1}
l	Meridional wavenumber	m^{-1}
K	Horizontal wavenumber	m^{-1}
ALE	Available latent energy	$J\ m^{-1}$
$\mathcal{A}$	Moisture mode activity	$J\ m^{-1}$
$\mathcal{G}$	ALE generation	$W\ m^{-1}$
$\mathcal{D}$	Moisture mode activity dissipation	$W\ m^{-1}$

We will modify the model of A21 to account for the presence of an idealized Hadley Cell, and examine motions under the WTG approximation, rather than the quasi-geostrophic approximation. For simplicity, we will consider the evolution of motions on an f-plane. Readers interested in how the system behaves on a beta plane are referred to supplementary information (SI) section 1. The layout of the model is shown schematically in Fig. 2. The idealized Hadley Cell is comprised of equatorward and easterly winds in the lower troposphere and poleward and westerly winds in the upper troposphere. The equatorward side of Cell is ascending and humid, while the poleward side is descending and dry. Since we are interested in understanding the interactions between waves

Accepted for publication in *Journal of Climate*. DOI 10.1175/JCLI-D-23-0147.1.

TABLE 2. Constants and their values.

Var.	*Description*	*Units*
C_p	Specific heat at constant pressure	1004 J kg^{-1} K^{-1}
R_d	Dry gas constant	287 J kg^{-1} K^{-1}
L_v	Latent heat of vaporization	2.5×10^6 J kg^{-1}
L_H	Hadley Cell half width	1000 km
Δp	Atmosphere half depth	500 hPa
f_0	Planetary vorticity	3×10^{-5} s^{-1}
S	Gross dry stability	1.25×10^8 J m^{-2}
c	Free gravity wave phase speed	58 m s^{-1}
L_d	Rossby radius of deformation	2×10^6 m
ϵ_1	Upper troposphere dissipation coefficient	1×10^{-6} s^{-1}
ϵ_3	Lower troposphere dissipation coefficient	2×10^{-6} s^{-1}
τ_c	Domain-mean convective moisture adjustment timescale	4 days
$L_v[\overline{E}]$	Domain-mean latent heat flux	100 W m^{-2}
R_{cs}	Column radiative cooling rate	110 W m^{-2}
$[\overline{W}]$	Domain-mean column moisture	40 kg m^{-2}
$\partial_y \overline{W}$	Zonal-mean column moisture gradient	10^{-5} kg m^{-3}
β_q	Mean meridional moisture gradient (in units of vorticity gradient)	1×10^{-11} (m s)$^{-1}$
l	First meridional wavenumber	1.5×10^{-6} m^{-1}

and the Hadley Cell in isolation, we will bind our model with rigid walls at a distance L_H from the center of the domain.

As in A21, we will assume that the vertical velocity (ω) attains a maximum amplitude in layer 2, and becomes zero at the top and bottom boundaries. For simplicity, we assume that ω increases linearly from p_0 to p_2, and decreases linearly thereafter. As a result, ω_3 can be written in terms of ω_2 as:

$$\omega_1 = \omega_3 = \frac{\omega_2}{2}. \tag{1}$$

By assuming that ω has a simple structure, we can invoke mass continuity in each discrete layer in order to relate it to the horizontal divergence (δ). Hence, we can write the divergence in layers 1 and 3 as:

$$\delta_3 = \frac{\omega_2}{\Delta p} \qquad\qquad \delta_1 = -\delta_3 \tag{2}$$

where Δp is half the depth of the atmosphere in this model.

Accepted for publication in *Journal of Climate*. DOI 10.1175/JCLI-D-23-0147.1.

Many of the variables used here will be column integrated, zonally averaged, and/or meridionally-integrated. For any variable X, these operations are defined as:

$$\langle X \rangle = \frac{1}{g} \int_{p_0}^{p_4} X dp \tag{3a}$$

$$\overline{X} = \frac{1}{2\pi a \cos\varphi} \oint X dx \tag{3b}$$

$$[X] = \int_{-L_H}^{L_H} X dy \tag{3c}$$

where $a = 6378$ km is the radius of the Earth, and $\varphi = 10°$N is our reference latitude. Deviations from this zonal average will be denoted as primes, i.e:

$$X' = X - \overline{X}. \tag{4}$$

The column integration will allow us to represent the apparent heating and moisture sink, Q_1 and Q_2 respectively, in terms of surface processes and column radiative heating. Following Yanai et al. (1973), we can column integrate Q_1 and Q_2, yielding:

$$\langle Q_1 \rangle = L_v P + \langle Q_r \rangle \tag{5}$$

$$\langle Q_2 \rangle = L_v (P - E) \tag{6}$$

where P is the surface precipitation rate, E is the surface evaporation, and $\langle Q_r \rangle$ is the column radiative heating rate. The $\langle Q_r \rangle$ is decomposed into a cloud-radiative heating component and a clear-sky radiative cooling R_{cs}:

$$\langle Q_r \rangle = r L_v P - R_{cs} \tag{7}$$

where r is the cloud-radiative feedback parameter (Peters and Bretherton 2005) or the greenhouse enhancement factor (Kim et al. 2015). Note that the effect of water vapor on radiative heating is implicitly included in r.

We will assume that precipitation is solely dependent on column integrated water vapor ($W = \langle q \rangle$, where q is the specific humidity). We will do a Taylor series expansion centered at $P = [\overline{P}]$, yielding:

Accepted for publication in *Journal of Climate*. DOI 10.1175/JCLI-D-23-0147.1.

$$P = [\overline{P}] + \frac{W - [\overline{W}]}{\tau_c} \tag{8a}$$

where

$$\tau_c = \left(\frac{\partial P}{\partial W}\right)^{-1} \tag{8b}$$

is a convective moisture relaxation timescale. While the relationship between P and W is nonlinear (Bretherton et al. 2004), we will use a constant value of τ_c to obtain simpler results. We have found that a value of τ_c of 4 days yields a reasonably realistic mean state in this model. This timescale is much larger than what empirical data suggests (Bretherton et al. 2004; Rushley et al. 2018; Adames et al. 2017). However, it is important to note that the τ_c is usually defined for regions of high precipitation, not for the tropical average. While the large and fixed value of τ_c is a limitation of this study, our main findings are not sensitive to the value of τ_c that is chosen for the analysis.

b. Domain means

Let us assume that our domain is in radiative-convective equilibrium (Manabe and Strickler 1964) and has a balanced hydrologic cycle. As a result, the domain-averaged balances in the thermodynamic and moisture equations are:

$$L_v[\overline{P}](1+r) = R_{cs} \tag{9a}$$

$$[\overline{P}] = [\overline{E}]. \tag{9b}$$

Assuming that $L_v[\overline{P}] = 100$ W m^{-2} yields a radiative cooling rate of 110 W m^{-2}, assuming that $r = 0.1$.

We posit that the equatorward edge of the Hadley Cell has a lapse rate that is roughly a moist adiabat, as in Emanuel (2019). Because the domain is in WTG balance, gravity waves will transmit this lapse rate to the rest of the domain. Assuming that layer 0 is dry and that layer 4 roughly corresponds to the boundary layer, we find that the domain-mean vertical change in DSE is equal to the boundary layer latent energy evaluated at $-L_H$:

$$[s_0] - [s_4] = L_v q_4(-L_H) \tag{10}$$

Accepted for publication in *Journal of Climate*. DOI 10.1175/JCLI-D-23-0147.1.

where $s = C_p T + \Phi$ is the dry static energy, T is the temperature and Φ is the geopotential. If $W = q_3 \Delta p / g$ is 50 mm at $-L_H$[1], and approximating $q_4 \simeq 2q_3$, we find that $\overline{q}_4 \simeq 0.02$, a value often seen near the surface of tropical oceans (Ciesielski et al. 2003; de Szoeke 2018). Using this value we find that $[s_0] - [s_4] = 5 \times 10^4$ J kg^{-1}.

c. Zonal mean state

The rising and sinking branches of the Hadley Cell are determined by the values of $\overline{W}$, which is assumed to decrease linearly with increasing y:

$$\overline{W}(y) = [\overline{W}] + y \frac{\partial \overline{W}}{\partial y}, \tag{11}$$

where $\partial_y \overline{W}$ is treated as a constant.

In Fig. 3a we show the meridional profile of $L_v \overline{W}$ for the two layer-model. For reference, the values of annual-mean $L_v W$ from ERA5 (Hersbach et al. 2020) is also shown for a domain that is comparable to that of the two-layer model. Further description of the ERA5 data is found in the caption of Fig. 3. This domain extends from the ITCZ to near the poleward edge of the tropics. The chosen linear profile of $L_v W$ reasonably represents the moisture decrease from the ITCZ near 7°N to the domain's edge near 25°N.

As in Polvani and Sobel (2002), we assume that the Hadley Cell is approximately in WTG balance so that our zonal-mean thermodynamic balance is:

$$-\overline{\delta}_3 S = L_v \overline{P}(1 + r) - R_{cs} \tag{12}$$

where

$$S = ([\overline{s}_0] - [\overline{s}_4]) \frac{\Delta p}{2g} \tag{13}$$

is the gross dry stability, defined as in Yu et al. (1998) and treated here as a positive constant. Because we are assuming that the zonal-mean meridional moisture gradient is constant, it follows that the mid-level vertical velocity changes linearly with latitude, as shown in Fig. 3b. This profile qualitatively captures the corresponding midtropospheric $\overline{\omega}$ in ERA5.

[1]This result is obtained by adding the average value of q between layers 2 and 3, and layers 3 and 4, respectively: $W = (q_3 + q_2)(p_3 - p_2)/(2g) + (q_4 + q_3)(p_4 - p_3)/(2g) = q_3 \Delta p / g$, recalling that $q_2 = 0$ and $q_4 = 2q_3$.

Accepted for publication in *Journal of Climate*. DOI 10.1175/JCLI-D-23-0147.1.

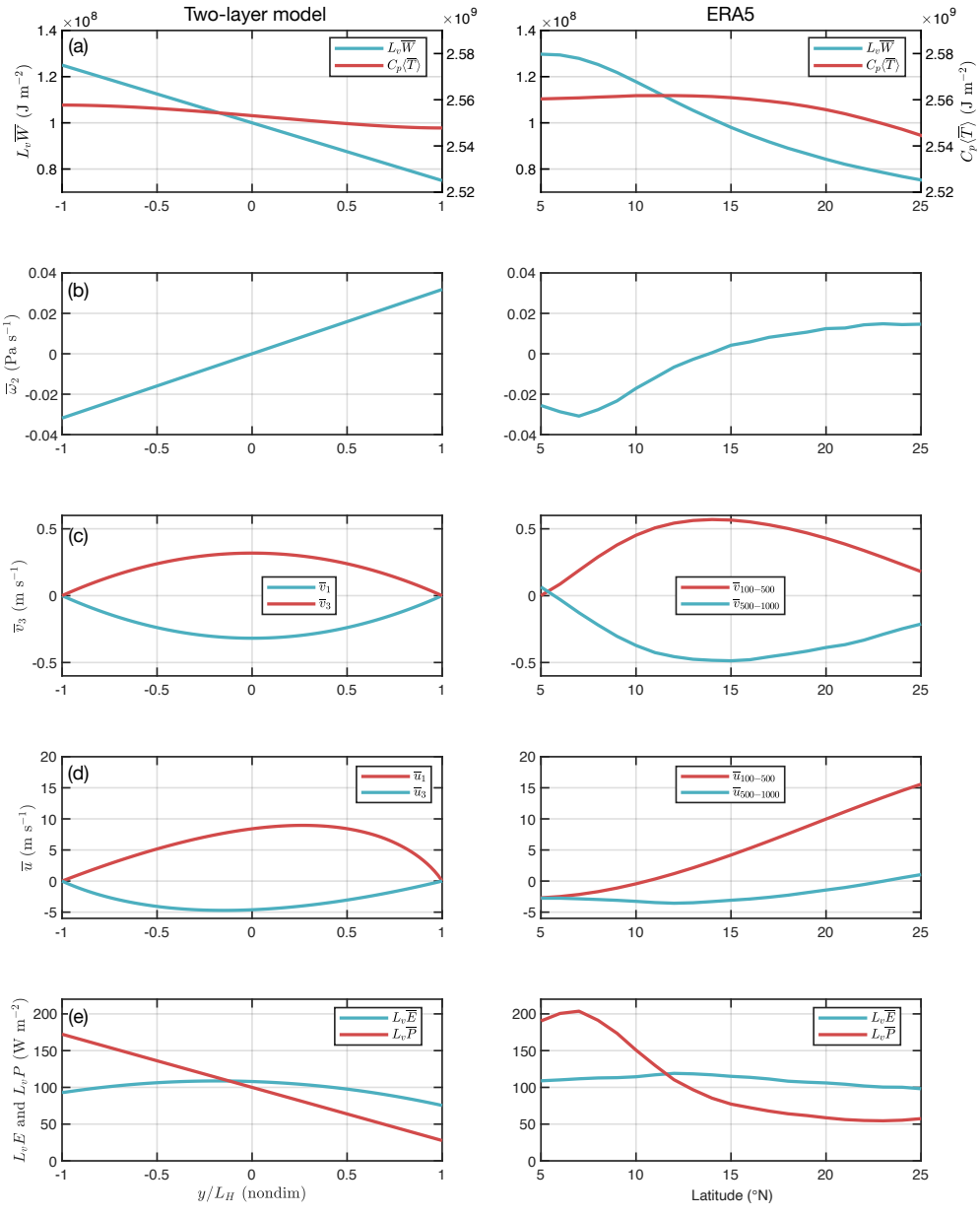

FIG. 3. Meridional profile of (a) $L_v(\overline{W}-[\overline{W}])$ (blue) and $C_p(\langle\overline{T}-[\overline{T}]\rangle)$ (red), (b) $\overline{\omega}_2$, (c) $\overline{v}_3$, (d) $\overline{u}_3$ (blue) and $\overline{u}_1$ (red), and (e) L_vE (blue) and L_vP (red) for the two-layer model (left) and for ERA5 data. We used monthly ERA5 data used is from 1979-2018, at a spatial resolution of $0.25°\times0.25$, and covering all available pressure levels from 100-1000 hPa. The shown profiles are averages of all 12 calendar months. Layer averages are denoted as subscripts for the indicated fields, which are chosen to best represent the corresponding layers of the idealized model.

Accepted for publication in *Journal of Climate*. DOI 10.1175/JCLI-D-23-0147.1.

By making use of Eq. (9a), and noting that $\overline{\delta}_3 = \partial_y \overline{v}_3$, we integrate Eq. (12) meridionally to obtain:

$$\overline{v}_3 = \overline{v}_0 \left(1 - \frac{y^2}{L_H^2}\right) \tag{14a}$$

where L_H is the Hadley Cell half-width, assumed constant, and $\overline{v}_0$ is the meridional wind over the reference latitude:

$$\overline{v}_0 = \frac{L_H^2(1+r)}{2S\tau_c} \frac{\partial L_v \overline{W}}{\partial y} \tag{14b}$$

Assuming that $L_H \simeq 1000$ km, and $\partial_y \overline{W} = -10$ mm per 1000 km we find that $\overline{v}_0 = -0.4$ m s^{-1}. In Fig. 3b we see that $\overline{v}_3$ is strongest over the reference latitude, and decreases to zero at $\pm L_H$. The parabolic profile of $\overline{v}$ is similar to that seen in both upper and tropospheric $\overline{v}$ seen in ERA5, although the latter attains a larger amplitude than that seen in the two-layer model.

We will assume that zonal momentum balance in the Hadley Cell is characterized by a balance between the Coriolis force, meridional zonal momentum advection and friction:

$$\overline{v}_3 \left(f_0 - \frac{\partial \overline{u}_3}{\partial y}\right) = \epsilon_3 \overline{u}_3, \tag{15a}$$

and geostrophic balance in the meridional momentum equation

$$f_0 \overline{u}_3 = -\frac{\partial \Phi_3}{\partial y} \tag{15b}$$

where ϵ is the dissipation coefficient. These momentum balances are similar to the WTG Hadley Cell model of Polvani and Sobel (2002). In this study, we will use a value of $\epsilon_1 = 1 \times 10^{-6}$ s^{-1} for the upper troposphere and $\epsilon_3 = 2 \times 10^{-6}$ s^{-1} for the lower troposphere. These values of ϵ_1 and ϵ_3 correspond to dissipation timescales of 11.6 days and 5.8 days, respectively, within the range of what previous studies have used (see Table 1 in Kim and Zhang 2021). In SI section 2 we discuss the sensitivity of the mean state to various values of ϵ.

In Fig. 3d we see that $\overline{u}_1$ has a maximum that is displaced north of the reference latitude, while u_3 is displaced slightly south. The $\overline{u}_3$ resembles the observed trade winds, peaking at 4 m s^{-1}. However, $\overline{u}_1$ does not resemble observed upper tropospheric winds, which increase until reaching a maximum value at the subtropical jet stream, consistent with the notion of approximate angular momentum conservation in the upper tropospheric branch of the Hadley Cell (Schneider 1977;

Accepted for publication in *Journal of Climate*. DOI 10.1175/JCLI-D-23-0147.1.

Held and Hou 1980). This disagreement is a result of the value of ϵ used and the application of rigid walls at the edges of the Hadley Cell. Decreasing ϵ will increase the upper tropospheric winds and accentuate a jet stream at the poleward edge of the Hadley Cell, but will also increase the meridional temperature gradient (SI section 2).

We can now use (15b) to obtain the thermal wind relation, which takes the following form in this model:

$$\frac{\partial \overline{T}_2}{\partial y} = \frac{f_0}{R_d}(\overline{u}_3 - \overline{u}_1) \tag{16}$$

using the zonal winds shown in Fig. 3d and using a reference latitude of 10°N, we find that the mean meridional temperature gradient is on the order of $\sim$ 1 K per 1000 km. When compared to the mean moisture gradient we see that the temperature gradient is roughly 6 times weaker (Fig. 3a). In ERA5 data we also see that the W gradient is much steeper than the temperature gradient, although the gradient is flatter on the equatorward edge and steeper at the poleward end of the domain.

Lastly, in order to balance the moisture budget, we diagnose the mean surface evaporation as:

$$\overline{E} = \overline{P} + \frac{\partial \overline{v}_3 \overline{W}}{\partial y}. \tag{17}$$

The resulting meridional profile of $\overline{E}$ has a maximum near the center of the domain, qualitatively resembling the reanalysis (Fig. 3e).

d. Simplified basic equations

We can substantially simplify the model of A21 if the following conditions are satisfied for the motions of interest.

1. *Thermodynamic variations are in WTG balance*. Following Charney (1963); Sobel et al. (2001) and Adames (2022), WTG balance is satisfied when:

$$\mathrm{N}_w = \frac{L_y^2}{L_d^2} \ll 1 \tag{18}$$

Accepted for publication in *Journal of Climate*. DOI 10.1175/JCLI-D-23-0147.1.

where L_y is the meridional scale of the system, and

$$L_d = \frac{c}{f_0} \qquad\qquad c = \left(\frac{R_d \Delta s}{2C_p}\right)^{\frac{1}{2}} \tag{19}$$

where L_d is the Rossby deformation radius, and c is the gravity wave phase speed. As we will show below, the meridional scale of the motion is determined by L_H, and the largest value that L_y can take is $2L_H/\pi \sim 6.4\times10^5$ m. For the motions we are interested in, we find that $\mathrm{N}_w \sim 0.1$.

2. *Moisture modes are the main synoptic-scale motion.* Ahmed et al. (2021); Mayta et al. (2022), and Adames (2022) showed that WTG balance is not a sufficient requirement to consider a system as a moisture mode. Another requirement is that $L_v W$ must govern the distribution of anomalous column moist enthalpy ($L_v W' + C_p\langle T'\rangle$). A small value of N_{mode} implies that $|L_v W'| \gg |C_p\langle T'\rangle|$. Since we are considering motions at high moisture values, it is convenient to define N_{mode} following Adames et al. (2019)

$$\mathrm{N}_{mode} = \frac{L_x}{\overline{u}_3 \tau_c}\mathrm{N}_w \ll 1 \tag{20}$$

Plugging in all the defined values yields $\mathrm{N}_{mode} \sim 0.02$.

With the two conditions satisfied, the basic equations in the two-layer model are written as:

$$\frac{\partial \zeta_1}{\partial t} = -\mathbf{v}_1 \cdot \boldsymbol{\nabla}_h \zeta_1 - (\zeta_1 + f_0)\delta_1 - \epsilon_1 \zeta_1 \tag{21a}$$

$$\frac{\partial \zeta_3}{\partial t} = -\mathbf{v}_3 \cdot \boldsymbol{\nabla}_h \zeta_3 - (\zeta_3 + f_0)\delta_3 - \epsilon_3 \zeta_3 \tag{21b}$$

$$-\delta_3 S = L_v P(1+r) - R_{cs} \tag{21c}$$

$$\frac{\partial W}{\partial t} = -\boldsymbol{\nabla}_h \cdot (\mathbf{v}_3 W) - P + E \tag{21d}$$

where the numbered subscripts indicate the layer of the variable as indicated in Fig. 2. Note that these equations neglect the contribution from vertical vorticity advection and vortex tilting in the evolution of vorticity. These terms were not included in the A21 model since they are negligibly small in the motions that the model is used to describe.

Accepted for publication in *Journal of Climate*. DOI 10.1175/JCLI-D-23-0147.1.

When examining Eq. (21), we see that all the information necessary to understand the evolution of the system is contained in Eqs. (21b)-(21d). The upper-tropospheric vorticity does not play a role in the evolution of ζ_3 and W. Hence, we will drop it and note that it is still used to determine the vertical structure of the resulting waves. Thus, we can combine Eqs. (21b)-(21d) to obtain the following equations vorticity and moisture:

$$\frac{\partial \zeta_3}{\partial t} = -\mathbf{v}_3 \cdot \boldsymbol{\nabla}_h \zeta_3 - \frac{\zeta_3 + f_0}{S}\left(\frac{L_v(W - [\overline{W}])}{\tau_c}\right)(1+r) - \epsilon_3 \zeta_3 \tag{22a}$$

$$\frac{\partial W}{\partial t} = -\mathbf{v}_3 \cdot \boldsymbol{\nabla}_h W + C \tag{22b}$$

where

$$C = -\left(1 - \frac{L_v W}{S}(1+r)\right)P - \frac{W}{S}R_{cs} + E \tag{23}$$

is the so-called column process (Chikira 2014). It is worth noting that $L_v W/S$ is the so-called Chikira parameter α, while $1 - L_v W/S$ is similar to the so-called "gross moist stability" (Neelin and Held 1987).

There are three processes on the right-hand side (rhs) of Eq. (22a): horizontal vorticity advection, vortex stretching and frictional dissipation. There are four processes on the rhs of Eq. (22b): horizontal moisture advection and three column processes: vertical MSE advection by convection (including cloud-radiative feedbacks), vertical moisture advection by clear-sky radiative cooling and surface evaporation.

3. Linear wave solutions

a. Linearization and scaling

We will now linearize Eq. (22) with respect to the idealized Hadley Cell. Following conventional linearization procedures, we will assume that the perturbations fields are much smaller amplitude than the zonal-mean values. This assumption allows the resulting equations to be analytically solvable. Furthermore, since the lower tropospheric winds are weak, it follows that ζ_3 is much smaller than f_0 over most of the domain. Given that the perturbations in vorticity are much smaller than the mean values, we can simplify $(f_0 + \zeta_3) \simeq f_0$ in Eq. (22a). These assumptions and

Accepted for publication in *Journal of Climate*. DOI 10.1175/JCLI-D-23-0147.1.

approximations lead to the following pair of linearized equations:

$$\frac{\overline{D}_h \zeta_3'}{Dt} = -\frac{f_0}{S\tau_c} L_v W'(1+r) \tag{24a}$$

$$\frac{\overline{D}_h W'}{Dt} = -v_3' \frac{\partial \overline{W}}{\partial y} - \frac{\Gamma_e W'}{\tau_c} + E' \tag{24b}$$

where

$$\frac{\overline{D}_h}{Dt} = \frac{\partial}{\partial t} + \overline{\mathbf{v}}_3 \cdot \boldsymbol{\nabla}_h \tag{25}$$

is the material derivative following the mean horizontal flow, and

$$\Gamma_e = 1 - \frac{L_v}{S}\left([\overline{W}] + 2y\frac{\partial \overline{W}}{\partial y}\right)(1+r) \tag{26}$$

is the mean effective gross moist stability (Sobel and Maloney 2013), a measure of the mean stability that includes the impact of radiative heating. Note that in deriving Eq. (26) we have made use of Eqs. (8) and (12) to eliminate R_{cs} from the moisture budget. It is also worth nothing that the last two terms on the rhs of Eq. (24b) are the anomalous column processes ($C' = -\Gamma_e W'/\tau_c + E'$).

Over the entirety of our idealized Hadley Cell $|\overline{u}| \gg |\overline{v}|$, allowing us to drop the advection by $\overline{v}$ in our equations so long as the meridional scale of our wave solutions is similar to or larger than its zonal scale ($L_y \geq L_x$). This is a reasonable approximation since $L_y \sim L_x$ for the two conditions outlined above to be valid.

As in Sobel et al. (2001), we decompose the horizontal winds into irrotational and non-divergent components. In the case when the frequency of the wave relative to the mean flow is small compared to f_0, the nondivergent wind will be much stronger than the irrotational wind (Eq. 37 in Sobel et al. 2001). This approximation is obtained from Eq. (29a) from the following condition:

$$\zeta' \sim f_0 \tau_d \delta' \tag{27}$$

where τ_d is the timescale of the wave relative to the mean flow, i.e., the Doppler-shifted timescale. If $f_0\tau_d \gg 1$ it follows that $|\zeta'| \gg |\delta'|$. Thus, we can write the anomalous horizontal winds in terms

Accepted for publication in *Journal of Climate*. DOI 10.1175/JCLI-D-23-0147.1.

of a streamfunction (ψ'):

$$u' \simeq -\frac{\partial \psi'}{\partial y} \qquad\qquad v' \simeq \frac{\partial \psi'}{\partial x} \tag{28}$$

recalling that $\zeta' = \nabla_h^2 \psi'$.

We are particularly interested in the special case when the meridional advection of mean moisture by v' governs $\overline{D}_h W'/Dt$. This occurs when the meridional moisture gradient is large enough that $|v'\partial_y \overline{W}|$ is much larger than E'. Additionally, τ_d must be on the order of 10^6 days and Γ_e must be much smaller than unity for $|v'\partial_y \overline{W}| \gg |\Gamma_e W'/\tau_c|$. For Γ_e to be small, the environment must be humid and cloud-radiative feedbacks sufficiently strong to offset any large-scale drying driven by convection. These conditions are discussed in more detail in SI section 4. While we note that these conditions are not necessarily realistic, they will allow us to investigate instabilities driven by horizontal moisture advection in isolation.

With these assumptions and approximations, our linearized system of equations is written as:

$$\frac{\partial \zeta_3'}{\partial t} = -\overline{u}_3 \frac{\partial \zeta_3'}{\partial x} + \frac{f_0}{S}\frac{L_v W'}{\tau_c}(1+r) \tag{29a}$$

$$\frac{\partial W'}{\partial t} = -\overline{u}_3 \frac{\partial W'}{\partial x} - v_3' \frac{\partial \overline{W}}{\partial y} \tag{29b}$$

This system closely resembles the one depicted in Sobel et al. (2001). They differ in the fact that the waves are bounded by rigid walls at $\pm L_H$ and that the Γ_e term is dropped.

b. Necessary conditions for instability

Before we pursue analytical solutions to Eq. (29), it is instructive to examine the conditions in which waves within our idealized Hadley Cell are unstable. Following Charney and Stern (1962), we assume that wave solutions exist of the form:

$$\psi'(x,y,t) = \mathrm{Re}[\tilde{\psi}(y)\exp(ikx - i\varpi t)] \tag{30}$$

$$W'(x,y,t) = \mathrm{Re}[\tilde{W}(y)\exp(ikx - i\varpi t)] \tag{31}$$

Accepted for publication in *Journal of Climate*. DOI 10.1175/JCLI-D-23-0147.1.

where k is the zonal wavenumber, ϖ is the wave frequency, and $\tilde{\psi}$ and $\tilde{W}$ are complex initial amplitudes.

From here on, we combine Eqs. (29a)-(29b) into a single equation. Afterwards, we multiply the equation by the complex conjugate of $\tilde{\psi}$, and meridionally integrate, assuming that $\psi' \to 0$ at the boundaries. This is the same procedure done by Charney and Stern (1962). Doing so yields the following condition for the imaginary component of the resulting equation:

$$\int_{-L_H}^{L_H} \frac{\left(\varpi_{rd}^2 - \varpi_i^2\right)}{(\varpi_{rd}^2 + \varpi_i^2)^2} \frac{f_0}{\tau_c} \frac{\partial \overline{W}}{\partial y} |\tilde{\psi}|^2 dy = 0 \tag{32}$$

where we have decomposed the wave frequency into real and imaginary parts ($\varpi = \varpi_r + i\varpi_i$), defining $\varpi_{rd} = \varpi_r - \overline{u}_3 k$ as the Doppler-shifted real component of the frequency. Here ϖ_r is the contribution to the propagation, while ϖ_r describes the growth rate.

From an examination of Eq. (32), we see that if ϖ_{rd} is nonzero then ϖ_i must also be nonzero for the integral to vanish. Either $\varpi_{rd}^2 = \varpi_i^2$ over the entire domain or $\varpi_{rd}^2 - \varpi_i^2$ changes sign somewhere in the domain. The former case occurs when $\overline{u}_3$ is a constant and the latter when it varies meridionally. Other terms in the integral are either constants or positive quantities in our idealized Hadley Cell and hence cannot make the integral vanish. As a result, waves that propagate relative to the mean flow within the idealized Hadley Cell are always unstable in the presence of rotation and a horizontal moisture gradient.

c. Dispersion relation

To elucidate the instability described by Eq. (32), we will now find analytical solutions to Eq. (29). The simplest solutions can be obtained if we replace $\overline{u}_3$ with its meridional-mean value ($[\overline{u}_3]$). This approximation is not accurate for the profile of $\overline{u}_3$ shown in Fig. 3, but we posit that the solutions that arise from it can still qualitatively describe the more general case in which $\overline{u}_3$ varies in latitude. By doing this replacement, the wave solutions take the following form:

$$\psi_3' = \mathrm{Re}[\tilde{\psi}_3 \cos(ly) \exp(ikx - i\varpi t)] \tag{33a}$$

$$W' = \mathrm{Re}[\tilde{W} \cos(ly) \exp(ikx - i\varpi t)] \tag{33b}$$

Accepted for publication in *Journal of Climate*. DOI 10.1175/JCLI-D-23-0147.1.

where l is the meridional wavenumber. Note that $\tilde{\psi}_3$ and $\tilde{W}$ are now complex constants rather than functions of latitude as in the previous subsection. They are related by the polarization relation:

$$\tilde{W} = \frac{k\partial_y \overline{W}}{\varpi - [\overline{u}_3]k}\tilde{\psi}_3. \tag{34}$$

Because rigid walls bound our domain at $\pm L_H$, it follows that the wave solutions have meridional structures that are restricted to oscillate an integer amount of times over twice the width of the Hadley Cell ($4L_H$). Thus, l is defined as:

$$l = \frac{(2\hat{l}-1)\pi}{2L_H} \qquad\qquad \hat{l} = 1, 2, 3...$$

By invoking Eq. (33) and substituting in Eq. (29) we obtain the dispersion relation

$$\varpi = [\overline{u}_3]k \pm \sqrt{\frac{i\beta_q k}{\tau_c K^2}} \tag{35a}$$

where $K^2 = k^2 + l^2$ is the horizontal wavenumber, and

$$\beta_q = -\frac{f_0}{S}\frac{\partial L_v \overline{W}}{\partial y}(1+r) \tag{35b}$$

is the mean meridional moisture gradient, expressed in the same units as β to facilitate its interpretation. Note that this definition differs from that of A21 as it is multiplied by $L_v W(1+r)/S$.

The dispersion relation in Eq. (35a) has two wave solutions, with one of them being unstable, as shown in Fig. 4. The square root term is equal parts real and imaginary since $\sqrt{i} = (1+i)/\sqrt{2}$. Hence, Eq. (35a) satisfies Eq. (32) by satisfying the condition $\omega_{rd} = \omega_i$. A close examination of Eq. (35a) shows that regardless of the sign of β_q, one of the wave solutions will always be unstable.

Two opposing processes contribute to the propagation of the wave. The first is advection by the mean lower-tropospheric winds, which act to propagate the system westward. The second is vortex stretching arising from meridional moisture advection. Lower tropospheric southerlies advect moist, precipitating air to the east of the wave center (bottom panel of Fig. 5). The vortex stretching associated with the advected air acts to propagate the wave eastward. From Fig. 4, we see that the latter process is dominant at small k. As k increases, the phase speed asymptotically

Accepted for publication in *Journal of Climate*. DOI 10.1175/JCLI-D-23-0147.1.

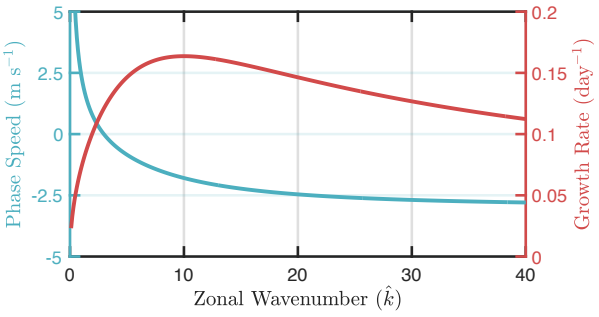

FIG. 4. Phase speed (blue) and growth rate (brown) of the unstable wave solution from Eq. (35).

approaches the $[\overline{u}_3]$ value of -3 m s^{-1}. One can interpret the growth of synoptic scale systems as propagation against the mean winds, akin to midlatitude Rossby waves, albeit in the opposite direction of motion.

Vortex stretching arising from meridional moisture advection is the only process that contributes to growth. Growth increases from wavenumber 1 and peaks near zonal wavenumber 10, decreasing afterward. It is worth pointing out that the instability is identical to the one that is obtained from Sobel et al. (2001) and Adames and Ming (2018) when the dispersion relation is not simplified. The main distinction is that the moistening is in the direction of propagation relative to the mean flow. In the case we are considering, the waves are traveling eastward relative to the mean easterly winds. Thus, these systems grow from MVI.

In Fig. 5 we see that the growing mode exhibits a horizontal structure that is mostly confined to the lower troposphere. Little signature is seen in the upper troposphere. The positive W and hence the P anomalies are shifted to the east of the center of low pressure (ψ_3' minimum). Because the P anomalies are shifted east of, but not in quadrature with ψ_3', it follows that the P anomalies are contributing to both the propagation and growth of the system, as Eq. (35a) indicates.

When examining the column-integrated moisture budget of the growing waves, which is equivalent to their MSE budget under WTG balance, we see that the fastest-growing zonal scale propagates westward nearly entirely from advection by the mean zonal winds (top panel in Fig. 6). They grow from meridional advection of mean moisture (bottom panel in Fig. 6), as was found for many TD-like and equatorial Rossby waves in MA.

Accepted for publication in *Journal of Climate*. DOI 10.1175/JCLI-D-23-0147.1.

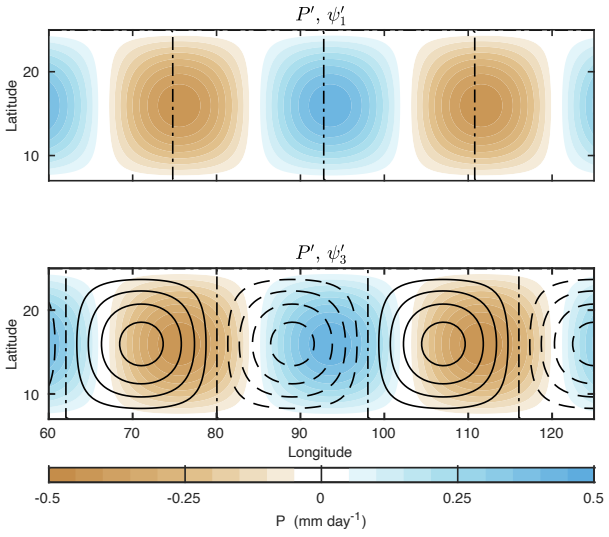

FIG. 5. Streamfunction anomalies of the growing wave solution from Eq. (35) in upper (layer 1, top) and lower troposphere (layer 3, bottom). The figure is constructed for zonal wavenumber 10 and the latitudes qualitatively represent the width of the Hadley Cell. The lower troposphere structure is obtained using Eq. (34). A similar procedure is used to obtain the upper-tropospheric structure. In both panels, P' is shown in shading. Contour interval 0.5×10^5 m^2 s^{-1}.

4. Moisture mode-Hadley Cell interactions mediated by moisture transports

a. Moisture mode activity

We now return to the basic equations and consider interactions between the unstable wave solutions described in Eq. (32) and the mean state. As shown in Eq. (35) and Fig. 6, the growth of W' is largely determined by the meridional advection of $\overline{W}$ by v_3', a signature of MVI. This covariance between W' and v_3' will lead to increased moisture variance in the latitude band where the unstable waves are located. To elucidate this, we multiply Eq. (22b) by W' and zonally-average it, yielding a budget for the zonally-averaged column moisture variance:

$$\frac{1}{2}\frac{\partial \overline{W'^2}}{\partial t} = -\overline{v_3' W'}\frac{\partial \overline{W}}{\partial y}. \tag{36}$$

As suggested above, Eq. (36) shows that the moisture variance changes in time only when there is an eddy moisture flux downgradient of $\overline{W}$. A poleward flux of latent energy implies that MVI is occurring.

Accepted for publication in *Journal of Climate*. DOI 10.1175/JCLI-D-23-0147.1.

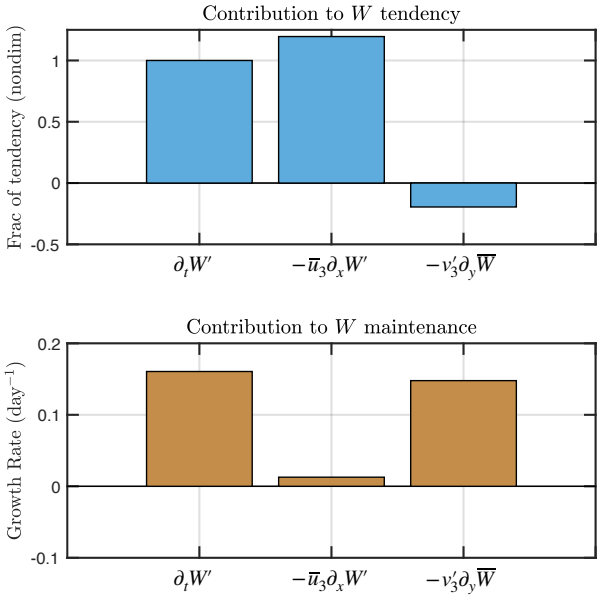

FIG. 6. Relative contribution of the two terms in Eq. (22b) to the (top) propagation and (bottom) growth of the W anomalies for growing wave shown in Fig. 5. The bars are projections of Eq. (22b) to the (top) $\partial_t W'$ and (bottom) W' following Eq. (5) in MA applied to our model domain.

The presence of eddy moisture fluxes will induce a zonal-mean moisture tendency through its meridional divergence:

$$\frac{\partial \overline{W}}{\partial t} = -\frac{\partial \overline{v_3' W'}}{\partial y}. \tag{37}$$

When examining Eqs. (36) and (37) we see that the term $\overline{v_3' W'}$ appears in both equations, implying that $\overline{W}$ and W' are coupled. Furthermore, when comparing with QG theory, we can see that Eq. (36) resembles, and behaves similarly to the QG enstrophy equation, while Eq. (37) resembles the mean-state PV budget (Vallis 2017).

As in QG wave-mean flow interactions, we can use Eq. (36) to obtain an equation that describes the evolution of wave activity within our idealized Hadley Cell. By dividing by $\partial \overline{W}/\partial y$ and assuming that it varies in time much more slowly than $\overline{W'^2}$, we obtain the following:

$$\frac{\partial \mathcal{A}}{\partial t} = L_v \overline{v_3' W'} \qquad\qquad \mathcal{A} = -\frac{L_v \overline{W'^2}}{2} \left(\frac{\partial \overline{W}}{\partial y} \right)^{-1} \tag{38}$$

Accepted for publication in *Journal of Climate*. DOI 10.1175/JCLI-D-23-0147.1.

where we define $\mathcal{A}$ as the moisture mode activity. Here we note the similarity of $\mathcal{A}$ to Rossby wave activity (see Ch 10 in Vallis 2017). We include a negative sign in the definition of $\mathcal{A}$ so that it is a positive quantity, recalling that the mean meridional moisture gradient is equatorward (negative).

In order to obtain an equation that mirrors Eq. (38) but for the mean state, we integrate Eq. (37) meridionally from $-L_H$ to y. Noting that there are no eddy moisture fluxes at the edges of the Hadley Cell, the resulting equation is written as:

$$\frac{\partial \mathrm{ALE}}{\partial t} = -L_v \overline{v_3' W'} \qquad\qquad \mathrm{ALE} = \frac{y^2 - L_H^2}{2} \frac{\partial L_v \overline{W}}{\partial y} \tag{39}$$

where we have defined a new variable, the "available latent energy" (ALE). Noting that the rhs of Eqs. (38) and (39) are equal and opposite, we can add them to obtain the conservation relation:

$$\frac{\partial}{\partial t} \left(\mathrm{ALE} + \mathcal{A} \right) = 0. \tag{40}$$

We can now use Eq. (40) to define the ALE as the amount of latent energy that is available to be converted to moisture mode activity $\mathcal{A}$. The magnitude of the ALE is directly proportional to the mean meridional moisture gradient. The naming ALE is opted to indicate that only the latent energy that is associated with the mean moisture gradient is available for the eddies to grow from MVI. ALE also describes the strength of the Hadley Cell. When ALE is higher, the ITCZ is more humid and rainier while the subsiding branch is drier.

The relationship in Eq. (40) implies that moisture modes in this model grow by extracting ALE via MVI and hence flattening the mean moisture gradient. Thus, the *moisture modes in this model grow at the expense of the Hadley Cell*.

This flattening effect can be seen more clearly if we invoke the flux-gradient hypothesis, i.e., $\overline{v_3' W'} = -\kappa_W \partial_y \overline{W}$, where κ_W is a moisture diffusivity. Using this approximation we can re-express Eq. (39) as:

$$\frac{\partial \mathrm{ALE}}{\partial t} = -\frac{\mathrm{ALE}}{\tau_D} \tag{41}$$

where $\tau_D = L_H^2/(2\kappa_w)$ is the ALE consumption timescale. Scaling of the definition of κ_w suggests that it is roughly 3×10^{-5} m^2 s^{-1}, a value similar to that found by Neelin and Zeng (2000). Using

Accepted for publication in *Journal of Climate*. DOI 10.1175/JCLI-D-23-0147.1.

this value we find that τ_D is roughly on the order of 20 days. Thus, while the consumption of ALE is slow compared to the timescale of the moisture modes, it is fast enough that it can have a significant impact at the intraseasonal timescale.

b. Mass streamfunction perspective

Many studies describe the overturning circulation associated with the Hadley Cell in terms of a mass streamfunction (Oort and Yienger 1996; Dima and Wallace 2003; Stachnik and Schumacher 2011), defined as:

$$\overline{\Psi} = \frac{2\pi a \cos\varphi}{g} \int_0^p \overline{v} dp. \tag{42}$$

As in previous studies (Oort and Yienger 1996; Caballero 2007), we can use the maximum value of $\overline{\Psi}$ ($\overline{\Psi}_{max}$) as a proxy of the strength of the Hadley Cell, which we obtain by evaluating it over the reference latitude at $p_2 = 500$ hPa. By combining Eq. (42) with Eq. (14) we obtain the following:

$$\overline{\Psi}_{max} = \frac{\Delta p}{g} \frac{2\pi a \cos\varphi}{S\tau_c} \mathrm{ALE}(1+r). \tag{43}$$

This expression explicitly shows that the strength of the overturning circulation is directly related to the ALE. If we combine it with Eq. (40) we find that

$$\frac{\partial \overline{\Psi}_{max}}{\partial t} = -\frac{\Delta p}{g} \frac{2\pi a \cos\varphi}{S\tau_c} (1+r) \frac{\partial \mathcal{A}}{\partial t}. \tag{44}$$

once again showing that increasing moisture mode activity weakens the overturning circulation.

c. Steady state interactions under the presence of dissipation

Up to this point, we have only considered how moisture modes evolve when only linear interactions between the mean state and the waves are allowed. However, MA found that nonlinear horizontal moisture advection is a significant MSE sink, damping both equatorial Rossby waves and TD-like waves at all times. However, the damping is stronger in TD-like waves. Given that TD-like waves are smaller in scale than their Rossby wave counterparts, it is fair to assume that the nonlinear horizontal advection arises from mesoscale processes that act as a moisture diffusion ($\kappa_W \nabla_h^2 W'$). For completeness, C' will also be included. As a result, the modified equation for $\mathcal{A}$

Accepted for publication in *Journal of Climate*. DOI 10.1175/JCLI-D-23-0147.1.

is written as:

$$\frac{\partial \mathcal{A}}{\partial t} = \overline{v_3' W'} - \mathcal{D} \tag{45a}$$

$$\mathcal{D} = -\frac{\kappa_W \overline{W' \nabla_h^2 W'}}{\partial_y \overline{W}} + \frac{\overline{\Gamma_e W'^2}}{\tau_c \partial_y \overline{W}} - \frac{\overline{E' W'}}{\partial_y \overline{W}} \tag{45b}$$

where $\mathcal{D}$ is defined as the dissipation of $\mathcal{A}$. If we no longer assume that Eq. (37) is satisfied for the zonal-mean state, then the budget for ALE becomes

$$\frac{\partial \mathrm{ALE}}{\partial t} = -\overline{v_3' W'} + \mathcal{G} \tag{46}$$

where we have grouped the terms in Eq. (37) into a single ALE generation term:

$$\mathcal{G} = \frac{L_v}{L_H} \int_{-L_H}^{y} \overline{C} dy \tag{47a}$$

where

$$\overline{C} = -\left(1 - \frac{L_v \overline{W}}{S}(1+r)\right) \frac{\overline{W}}{\tau_c} - \frac{\overline{W}}{S} R_{cs} + \overline{E} \tag{47b}$$

is the column process associated with the zonal-mean circulation.

In steady state, combining Eq. (46) with Eq. (45) leads to a balance between eddy dissipation and ALE generation:

$$\mathcal{D} = \mathcal{G}. \tag{48}$$

This result indicates that mean state motions amplify the moisture gradient. However, the mean state is unstable and the added ALE is quickly consumed by eddies, which then dissipate. Thus, *latent energy follows a direct energy cascade, as in kinetic energy*.

Furthermore, if we assume that the horizontal scale of the eddies remains fixed, we find that $\mathcal{D} \sim 2\kappa_W K^2 \mathcal{A}$, so that Eq. (48) also indicates that wave activity is proportional to $\mathcal{G}$.

From the perspective of Eq. (45), the steady state can be used to obtain a diagnostic equation for the precipitation variance:

$$\overline{P'^2} = -\frac{\overline{v_3' W'}}{\kappa_W K^2 \tau_c^2} \frac{\partial \overline{W}}{\partial y}. \tag{49}$$

Accepted for publication in *Journal of Climate*. DOI 10.1175/JCLI-D-23-0147.1.

This equation shows that precipitation variability is stronger along steeper gradient and with larger poleward eddy moisture fluxes, assuming that the other terms are fixed. Thus, while the ascending and descending branches of the Hadley Cell are steadily rainy and dry, respectively, the region in between is highly variable, fluctuating between rainy and dry periods associated with the passage of moisture modes.

From the perspective of the moisture budget, the balance of terms is written as:

$$\frac{\partial \overline{v_3' W'}}{\partial y} = \overline{C} \tag{50}$$

implying that the column processes of the Hadley Cell moisten the atmosphere, while the eddy transport dry it. This result is consistent with the findings Inoue et al. (2021), who found that horizontal moisture advection dries a precipitating column that would otherwise continue to moisten. We can show that our results agree with theirs by expanding the left-hand side of Eq. (50) using the product rule, yielding:

$$\overline{v_3' \frac{\partial W'}{\partial y}} = \frac{L_v \overline{W'^2}}{S\tau_c}(1+r) + \overline{C} \tag{51}$$

where the first term on the rhs is the eddy moisture convergence under WTG balance. Since it is a positive quantity it adds to $\overline{C}$. Hence only the nonlinear horizontal moisture advection dries the troposphere.

Energy transports in the Hadley Cell are usually examined using the MSE budget. With the inclusion of eddies, the budget takes the following form

$$L_v \frac{\partial \overline{v_3' W'}}{\partial y} = -\frac{\partial \overline{v}_3 \overline{m}}{\partial y} + L_v \overline{E} + \langle \overline{Q}_r \rangle \tag{52}$$

where we are showing the eddy contribution on the left-hand side and the Hadley Cell component on the rhs. Since the eddies are in WTG balance, it follows that their contribution to the MSE transport is governed by the latent energy component. As previously shown, $\overline{v_3' W'}$ must be poleward in order to balance the moisture diffusion, yielding a result that is consistent with the findings of Trenberth and Stepaniak (2003) and Rios-Berrios et al. (2020). Thus $\partial_y \overline{v_3' W'} > 0$ within the ITCZ, implying that the sum of the terms on the rhs of Eq. (52) must also be positive, which is in agreement with

Accepted for publication in *Journal of Climate*. DOI 10.1175/JCLI-D-23-0147.1.

Peters et al. (2008). Once again we find that the mean meridional moisture gradient would amplify in the absence of eddies.

Predator-prey cycles in moisture mode activity and Hadley Cell strength

We will now generalize the results of this section and consider the case in which moisture mode-Hadley Cell interactions occur with both changes in time and dissipation. Let us begin by assuming that the results of the previous subsection correspond to the climatology, and that small deviations from this climatology exist. As a result, we can decompose $\mathcal{A}$ and the ALE into climatological (denoted by curly brackets) and fluctuating components:

$$\mathcal{A} = \{\mathcal{A}\} + \mathcal{A}^+ \tag{53a}$$

$$\mathrm{ALE} = \{\mathrm{ALE}\} + \mathrm{ALE}^+. \tag{53b}$$

Let us consider the possibility that the moisture diffusivity κ_W is not a constant, but is instead proportional to $\mathcal{A}$. We reason this since $\overline{v'W'}$ is itself dependent on the strength of the moisture modes. Thus we write:

$$-\kappa_W \frac{\partial L_v \overline{W}}{\partial y} = \gamma \mathcal{A} \mathrm{ALE} \tag{54}$$

where γ is a constant with a rough value of 4×10^{-19} kg (m s)$^{-1}$, which we obtain from Table 2 and the scales discussed in Section 3.

Now let us consider the climatology. As in Inoue and Back (2017), we assume that $\overline{C}$ is proportional to the ALE itself. By invoking Eq. (41), we find that $\mathcal{G} \sim \mathrm{ALE}/\tau_D$. We can similarly assume that $\mathcal{D}$ is damping $\mathcal{A}$ via diffusion and from Γ_e being positive. Thus, it is reasonable to assume that $\mathcal{D} \sim -\mathcal{A}/\tau_D$. By making these approximations we find that the mean state balance is:

$$\{\mathcal{A}\} = \{\mathrm{ALE}\} \qquad\qquad \gamma\{\mathrm{ALE}\} = \tau_D^{-1} \tag{55}$$

Using Eqs. (53), (54), and (55) we can write Eqs. (45) and (46) as:

$$\frac{\partial \mathcal{A}^+}{\partial t} = \gamma\{\mathcal{A}\}\mathrm{ALE}^+ \tag{56a}$$

Accepted for publication in *Journal of Climate*. DOI 10.1175/JCLI-D-23-0147.1.

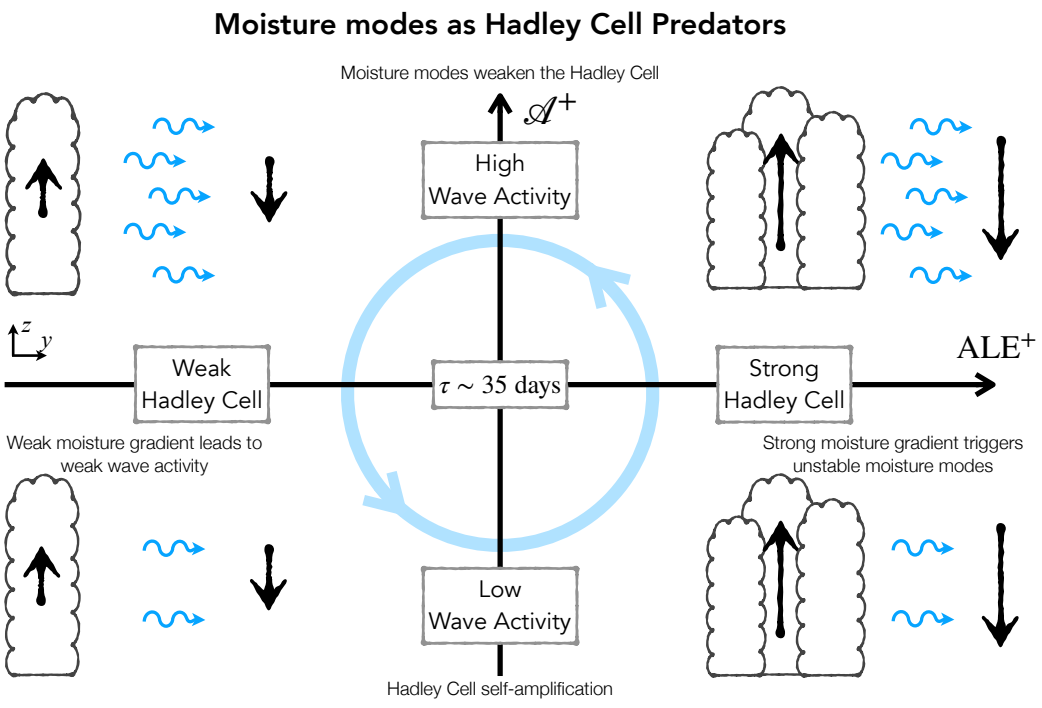

FIG. 7. Schematic describing the predator-prey relationship between moisture modes and the Hadley Cell according to the results of Section 4d. The x- and y-axis show ALE and wave activity ($\mathcal{A}$) deviations from climatology. The drawings in each quadrant depict the strength of the Hadley Cell (clouds) and the amount of wave activity (wavy arrows).

$$\frac{\partial \mathrm{ALE}^+}{\partial t} = -\gamma\{\mathrm{ALE}\}\mathcal{A}^+. \tag{56b}$$

Equation (56) is a linear predator-prey system similar to the one shown in Majda and Stechmann (2009). In this case the moisture modes behave as the predators and the Hadley Cell as the prey. The solution to this system is an oscillation with a frequency given by:

$$\varpi = \pm\gamma\{\mathrm{ALE}\} \tag{57}$$

A quick inspection of the definition of ALE suggests that it has a mean value of 10^{13} J m^{-1}. With the estimated value of γ we find that the oscillation has a timescale of ~35 days. Given that this value was derived from an estimation with a high degree of uncertainty, it is possible that this

Accepted for publication in *Journal of Climate*. DOI 10.1175/JCLI-D-23-0147.1.

value could vary by a factor of 2. Nonetheless, the oscillation would still occur at the intraseasonal timescale.

To qualitatively understand the nature of this predator-prey system, it is useful to invoke the chain rule $\frac{\partial \mathrm{ALE}^+}{\partial t} = \frac{\partial \mathrm{ALE}^+}{\partial \mathcal{A}^+}\frac{\partial \mathcal{A}^+}{\partial t}$, from which we obtain the following equality:

$$\mathrm{ALE}^{+2} + \mathcal{A}^{+2} = \text{constant}. \tag{58}$$

This result implies that there is a circular cycle in the ALE-$\mathcal{A}$ phase space. This cycle, shown in Fig. 7, implies that periods of high ALE are followed by periods of high wave activity. Since the wave activity reduces the ALE, the reverse part of the cycle ensues.

5. Discussion and Conclusions

a. Summary

In recent decades our understanding of tropical atmospheric motions has grown expeditiously (Emanuel 2018; Jiang et al. 2020; Adames and Maloney 2021). Part of this growth has been due to the increased awareness of the importance of water vapor in these motions (Held et al. 1993; Brown and Zhang 1997; Raymond 2000; Sobel et al. 2001; Wolding et al. 2020; Maithel and Back 2022, among others). As our understanding continues improving we have recognized that "moisture modes" may exist in the tropics (Yu and Neelin 1994; Fuchs and Raymond 2002). Initially used to describe the MJO (Raymond and Fuchs 2009; Sobel and Maloney 2013), recent studies have posited that moisture modes may be a more common feature of the tropics (Adames and Maloney 2021; Inoue et al. 2021; Maithel and Back 2022; Adames 2022). There is increasing evidence that convectively-coupled equatorial Rossby waves and tropical depression-like waves exhibit properties of moisture modes (Inoue et al. 2020; Gonzalez and Jiang 2019; Nakamura and Takayabu 2022a; Mayta et al. 2022).

On the basis of these findings, we investigated the possibility that moisture modes interact with the Hadley Cell. To do this, we employed the two-layer model of Adames (2021) and adapted it to accommodate an idealized Hadley Cell. The strength of the Hadley Cell is assumed to be proportional to the mean meridional moisture gradient. As in previous works (Charney 1963; Sobel

Accepted for publication in *Journal of Climate*. DOI 10.1175/JCLI-D-23-0147.1.

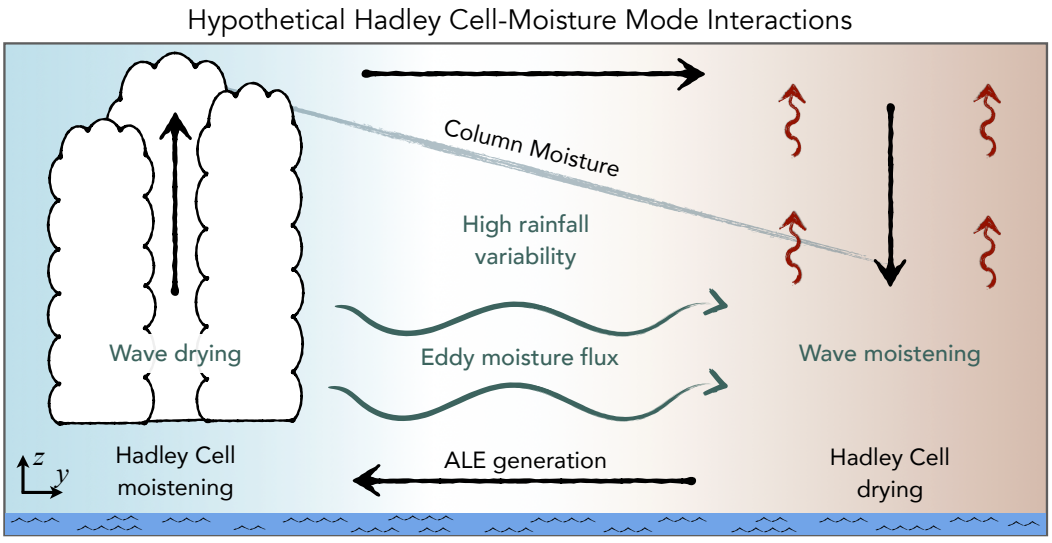

FIG. 8. As in Fig 2 but showing how moisture modes interact with the Hadley Cell according to the results of this study. The green wavy lines depict the eddy moisture flux and the light line above it shows the mean W distribution.

et al. 2001; Adames 2022), the overturning circulation is in WTG balance so long as the square of its meridional half-width (L_H^2) is smaller than the square of the Rossby radius of deformation (L_d^2).

If the mean state is simplified further by assuming the mean lower-tropospheric winds are constant, we obtain a system of equations that are nearly identical to those of Sobel et al. (2001), but with a restricted meridional scale. Wave solutions to this idealized mean state yield a pair of wave solutions, one of which is unstable. The unstable solution propagates westward from a combination of zonal advection by the mean flow and meridional advection of the mean moisture by the anomalous meridional winds. It is destabilized by the latter process. The most unstable wave grows near zonal wavenumber 10 and propagates westward at roughly the same speed as the trade winds.

An interesting result of Eq. (35) is that one of the wave solutions is always unstable, so long as the square root is nonzero. For example, a growing solution still exists if the moisture gradient is poleward, as we observe in the south Asian monsoon (Clark et al. 2020). This result means that a meridional moisture gradient in the presence of rotation (nonzero f) will always be unstable so long as convection is sensitive to water vapor fluctuations.

Accepted for publication in *Journal of Climate*. DOI 10.1175/JCLI-D-23-0147.1.

We then return to the original Hadley Cell model to examine if transients that grow from meridional moisture advection interact with the Hadley Cell. Our results show that moisture mode activity increases when there are poleward moisture fluxes. The pair of equations that describe the interaction between moisture modes and the Hadley Cell (Eqs. 38 and 39) are analogous to the Eliasen-Palm flux formulation (Andrews and Mcintyre 1976; Edmon Jr et al. 1980), with column water vapor taking the place of potential vorticity.

Examination of this pair of equations reveals that the eddy moisture fluxes flatten the mean meridional moisture gradient, therefore weakening the Hadley Cell, as summarized in Fig. 8. Conversely, a stronger ITCZ is associated with drier subtropics, consistent with previous work (Hohenegger and Jakob 2020; Popp et al. 2020). Furthermore, we found that the amplification of moisture modes at the expense of the Hadley Cell is transient, as the available latent energy (ALE) for moisture mode activity decreases with a weakening Hadley Cell. Such a transient behavior leads to a cycle, where moisture modes deplete the ALE and hence weaken the Hadley Cell, followed by a period of weak moisture mode activity where the Hadley Cell and the ALE rebuild. This oscillation occurs at the subseasonal timescale, and it is not clear if it may be associated with the MJO. It is, however, reminiscent of the ITCZ breakdown discussed by Ferreira and Schubert (1997). While we emphasize different mechanisms from theirs, it is possible that they are nonetheless related.

That the latent energy fluxes are poleward also suggests that they may be important for global energy transport. Eddy energy fluxes in the tropics are smaller than those in the midlatitudes, but they are not negligible (Fig. 1 in Trenberth and Stepaniak (2003) and Fig. 5 in Rios-Berrios et al. (2020)). Stoll et al. (2023) found that these fluxes correspond to synoptic-scale eddies (2,000-8,000 km across). In the tropics, eddy fluxes of energy are dominated by the latent energy component, with DSE transports being negligible, as would be expected from moisture modes.

b. MVI and the growth of TD-like waves

In spite being one of the most-well documented tropical transients, the key processes that drive the growth of TD-like waves remains a topic of extensive research (Lau and Lau 1992; Tam and Li 2006; Rydbeck and Maloney 2014; Alaka and Maloney 2014; Feng et al. 2016; Russell et al. 2020; Núñez Ocasio et al. 2020, among others). TD-like waves are observed in many areas of the world including, but not limited to, the northern Atlantic ocean, the northeast and northwest Pacific, and

Accepted for publication in *Journal of Climate*. DOI 10.1175/JCLI-D-23-0147.1.

over tropical Africa (Lau and Lau 1990; Kiladis et al. 2009, MA). Previous studies have suggested that these waves grow from barotropic, baroclinic, inertial instability, or a combination thereof that is amplified by deep convection (Lau and Lau 1992; Thorncroft and Hoskins 1994; Rydbeck and Maloney 2014; Torres et al. 2021). While our results do not reject the possibility that these processes are important, they hint at another potential explanation: TD-like waves are the result of the unstable horizontal moisture gradients that are present in the ITCZ and the monsoons. They may be fundamental features of the tropics as they may act to stabilize the Hadley Cell, preventing the moisture gradient along the flanks of the ITCZ from steepening. This is an attractive possibility since strong horizontal moisture gradients are common in the regions where TD-like waves are active (see Fig. 2 in MA). That the linear waves described here resemble observed TD-like waves supports this possibility, though more work is needed to further test it.

c. Potential relevance to tropical cyclones

The structure of the growing waves discussed here also bears resemblance to tropical cyclones (TCs). Both systems have circulations that are strongest in the lower troposphere, and water vapor plays an important role in the thermodynamic processes of both. In particular, it is well-known that free tropospheric moisture is important for TC genesis (Tang et al. 2016; Yoshida et al. 2017; Raymond and Kilroy 2019; Tang et al. 2020). Thus, it is possible that processes akin to MVI may be at play in TC formation. Such a possibility was hinted at by Narenpitak et al. (2020) and Núñez Ocasio and Rios-Berrios (2023). Narenpitak et al. (2020) found that flux of moisture towards the vortex center differentiated vortices that developed into TCs versus those that did not. While they did not mention it explicitly, developing waves exhibited properties of MVI. A qualitatively similar result was found by Núñez Ocasio and Rios-Berrios (2023) for an African easterly wave that developed into hurricane Helene. If TC development has elements of MVI in it, it is possible that the mechanisms described here also apply to TCs. This transport could occur in conjunction with the oceanic heat transport hypothesized by Emanuel (2001). This possibility should be examined in future work.

Accepted for publication in *Journal of Climate*. DOI 10.1175/JCLI-D-23-0147.1.

d. Potential relevance to convective self aggregation

An interesting interpretation of the results of this study comes from examining them from the perspective of convective self-aggregation (Bretherton et al. 2005; Wing and Emanuel 2014; Windmiller and Craig 2019). We can interpret the tendency of the Hadley Cell to amplify through column processes as a tendency for the ITCZ to aggregate through radiative-convective instability (Emanuel et al. 2014). In this case, the MSE/moisture variance in the ITCZ will increase, consistent with an increase in ALE. Under this lens, moisture mode activity would act to disaggregate the ITCZ by diffusing the moisture distribution. Maithel (2023) found that aggregation/disaggregation cycles exist in reanalysis, and are driven by horizontal MSE advection. Examining the results of this study from the view of aggregation could be a fruitful direction for future research.

e. Applicability to the Walker Cell

Extending these results to zonal moisture gradients can yield some interesting insights into the nature of Rossby waves and the MJO. Since the MJO is strongest over the Indian Ocean, a region characterized by an eastward and equatorward moisture gradient, it is possible that the MJO is diffusing latent energy from the Maritime Continent. Hence, the MJO moistens the Indian Ocean at the expense of moisture over the Maritime Continent. Some western Pacific equatorial Rossby waves may work analogously. Thus, both these systems would gain energy while weakening the Walker Cell.

f. Caveats

We acknowledge that the results of this study were obtained using an idealized two-layer model with several assumptions and approximations. Convection is parameterized as a linear function of column water vapor only. Focusing on water vapor allows makes our analysis more amenable for analytical interpretation. In observations, precipitation increases exponentially with increasing moisture, rather than linearly (Bretherton et al. 2004; Rushley et al. 2018). Additionally, large-scale convection also depends on fluctuations in temperature and vertical wind shear (Anber et al. 2016; Ahmed and Neelin 2018; Ahmed et al. 2020). The large-scale controls on deep convection is a topic of ongoing research (Schiro et al. 2018; Wolding et al. 2022), but we acknowledge that the simple representation of convection is a caveat of this study.

Accepted for publication in *Journal of Climate*. DOI 10.1175/JCLI-D-23-0147.1.

We also acknowledge that our mean state is highly idealized compared to observations. In observations, zonal and meridional asymmetries in the distribution of wind and moisture due to the presence of land masses can play an important role in the growth of tropical waves (Rydbeck et al. 2017; Feng et al. 2020a; Torres et al. 2021). While making these assumptions facilitates the analytical tractability of the model, they are another limitation of this study.

Another caveat of this study is that by assuming the motions exist within a Hadley Cell bounded by rigid walls we are neglecting the role the extratropics may have in determining the mean state in which the wave propagates. This assumption causes the winds to become zero at the edges of the Hadley Cell if friction is not ingnored, a feature that is inconsistent with observations. Furthermore, the two-layer model only accounts for the first baroclinic vertical motions. This was done since the oceanic TD-like waves that our study examines exhibit upright vertical velocities that are approximately first baroclinic (Serra et al. 2008; Inoue et al. 2020; Huaman et al. 2021). However, interactions between the first and second baroclinic mode can be important in TD-like waves (Núñez Ocasio et al. 2020; Russell et al. 2020; Torres et al. 2021). More work is needed to understand whether the results of this study are still valid in a more realistic setting.

g. Conclusions

We conclude this study by returning to the first paragraph of Section 1. Despite the acknowledgment that the tropics exhibit a diversity of motion systems, there is a lack of work done trying to understand how these systems interact with the mean circulation. Most studies assume the Hadley Cell to be a stable circulation and the most important source of energy transport out of the tropics. This study challenges this notion. Results from previous works (Inoue et al. 2021; Maithel and Back 2022, MA) suggest that horizontal moisture advection may be important in understanding rainfall variability and the growth of large-scale waves. Results from this work agree with these studies and reveal that horizontal moisture advection may play a central role in interactions between the Hadley Cell and the waves. These interactions are analogous to those of baroclinic eddies and the jet stream. While baroclinic instability weakens the jet stream by flattening the temperature gradient, moisture modes weaken the Hadley Cell by flattening the moisture gradient. These interactions are mediated by a poleward eddy moisture flux, which may play an important role in the global energy balance. If these results are confirmed by future studies, they would imply that

Accepted for publication in *Journal of Climate*. DOI 10.1175/JCLI-D-23-0147.1.

the diversity of weather systems seen in the tropics interact with the climate system in richer and more dynamic ways than previously thought.

Acknowledgments. ÁFAC was supported by NSF CAREER grant number 2236433, and by the University of Wisconsin startup package. VM was supported by NOAA grant number NA22OAR4310611. ÁFAC would like to thank his late father, Ángel David Adames Tomassini, for listening to and motivating him to complete this project in spite of strenuous circumstances. The contents of the manuscript were significantly improved after conversations with Rosimar Ríos Berríos and Rich Rotunno. We thank Haochang Luo for reviewing an early version of this manuscript. Lastly, we thank Adam Sobel and two anonymous reviewers for feedback and comments that helped improved the contents of the manuscript.

Data availability statement. ERA5 data is available at: `https://www.ecmwf.int/en/forecasts/datasets/reanalysis-datasets/era5/`). Interpolated T_b data are provided by the NOAA/ESRL.

References

Adames, Á. F., 2021: Interactions between water vapor, potential vorticity and vertical wind shear in quasi-geostrophic motions: Implications for rotational tropical motion systems. *Journal of the Atmospheric Sciences*, https://doi.org/10.1175/JAS-D-20-0205.1.

Adames, Á. F., 2022: The basic equations underweak temperature gradient balance: Formulation, scaling, and types of convectively-coupled motions. *Journal of the Atmospheric Sciences*.

Adames, Á. F., D. Kim, S. K. Clark, Y. Ming, and K. Inoue, 2019: Scale Analysis of Moist Thermodynamics in a Simple Model and the Relationship between Moisture Modes and Gravity Waves. *Journal of the Atmospheric Sciences*, **76 (12)**, 3863–3881, https://doi.org/10.1175/JAS-D-19-0121.1.

Adames, Á. F., D. Kim, A. H. Sobel, A. Del Genio, and J. Wu, 2017: Characterization of moist processes associated with changes in the propagation of the mjo with increasing co2. *Journal of Advances in Modeling Earth Systems*, **9 (8)**, 2946–2967, https://doi.org/10.1002/2017MS001040.

Accepted for publication in *Journal of Climate*. DOI 10.1175/JCLI-D-23-0147.1.

Adames, Á. F., and E. D. Maloney, 2021: Moisture Mode Theory's Contribution to Advances in our Understanding of the Madden-Julian Oscillation and Other Tropical Disturbances. *Current Climate Change Reports*, https://doi.org/10.1007/s40641-021-00172-4.

Adames, A. F., and Y. Ming, 2018: Interactions between Water Vapor and Potential Vorticity in Synoptic-Scale Monsoonal Disturbances: Moisture Vortex Instability. *Journal of the Atmospheric Sciences*, **75 (6)**, 2083–2106, https://doi.org/10.1175/JAS-D-17-0310.1.

Adames, Á. F., S. W. Powell, F. Ahmed, V. C. Mayta, and J. D. Neelin, 2021: Tropical precipitation evolution in a buoyancy-budget framework. *Journal of the Atmospheric Sciences*, **78 (2)**, 509 – 528, https://doi.org/10.1175/JAS-D-20-0074.1.

Ahmed, F., Á. F. Adames, and J. D. Neelin, 2020: Deep Convective Adjustment of Temperature and Moisture. *Journal of the Atmospheric Sciences*, **77 (6)**, 2163–2186, https://doi.org/10.1175/JAS-D-19-0227.1.

Ahmed, F., and J. D. Neelin, 2018: Reverse engineering the tropical precipitation–buoyancy relationship. *J. Atmos. Sci.*, **75 (5)**, 1587–1608, https://doi.org/10.1175/JAS-D-17-0333.1.

Ahmed, F., J. D. Neelin, and Á. F. Adames, 2021: Quasi-equilibrium and weak temperature gradient balances in an equatorial beta-plane model. *Journal of the Atmospheric Sciences*, **78 (1)**, 209–227.

Alaka, G. J., and E. D. Maloney, 2014: The intraseasonal variability of african easterly wave energetics. *Journal of climate*, **27 (17)**, 6559–6580.

Anber, U., S. Wang, and A. Sobel, 2016: Response of atmospheric convection to vertical wind shear: Cloud-system-resolving simulations with parameterized large-scale circulation. part ii: Effect of interactive radiation. *Journal of the Atmospheric Sciences*, **73 (1)**, 199–209.

Andersen, J. A., and Z. Kuang, 2012: Moist Static Energy Budget of MJO-like Disturbances in the Atmosphere of a Zonally Symmetric Aquaplanet. *J. Climate*, **25 (8)**, 2782–2804.

Andrews, D., and M. E. Mcintyre, 1976: Planetary waves in horizontal and vertical shear: The generalized eliassen-palm relation and the mean zonal acceleration. *Journal of Atmospheric Sciences*, **33 (11)**, 2031–2048.

Accepted for publication in *Journal of Climate*. DOI 10.1175/JCLI-D-23-0147.1.

Bretherton, C. S., P. N. Blossey, and M. Khairoutdinov, 2005: An energy-balance analysis of deep convective self-aggregation above uniform SST. *J. Atmos. Sci.*, **62 (12)**, 4273–4292.

Bretherton, C. S., M. E. Peters, and L. E. Back, 2004: Relationships between Water Vapor Path and Precipitation over the Tropical Oceans. *J. Climate*, **17**, 1517–1528.

Bretherton, C. S., and P. K. Smolarkiewicz, 1989: Gravity Waves, Compensating Subsidence and Detrainment around Cumulus Clouds. *J. Atmos. Sci.*, **46 (6)**, 740–759, https://doi.org/10.1175/1520-0469(1989)046⟨0740:GWCSAD⟩2.0.CO;2.

Brown, R. G., and C. Zhang, 1997: Variability of midtropospheric moisture and its effect on cloud-top height distribution during toga coare*. *J. Atmos. Sci.*, **54 (23)**, 2760–2774, https://doi.org/10.1175/1520-0469(1997)054⟨2760:VOMMAI⟩2.0.CO;2.

Caballero, R., 2007: Role of eddies in the interannual variability of hadley cell strength. *Geophysical Research Letters*, **34 (22)**.

Chang, C.-P., 1970: Westward propagating cloud patterns in the tropical pacific as seen from time-composite satellite photographs. *J. Atmos. Sci.*, **27 (1)**, 133–138, https://doi.org/10.1175/1520-0469(1970)027⟨0133:WPCPIT⟩2.0.CO;2.

Charney, J. G., 1963: A Note on Large-Scale Motions in the Tropics. *J. Atmos. Sci.*, **20 (6)**, 607–609.

Charney, J. G., and M. E. Stern, 1962: On the stability of internal baroclinic jets in a rotating atmosphere. *Journal of the Atmospheric Sciences*, **19 (2)**, 159–172.

Chen, G., 2022a: The amplification of madden–julian oscillation boosted by temperature feedback. *Journal of the Atmospheric Sciences*, **79 (1)**, 51–72.

Chen, G., 2022b: A model of the convectively coupled equatorial rossby wave over the indo-pacific warm pool. *Journal of the Atmospheric Sciences*, **79 (9)**, 2267–2283.

Chikira, M., 2014: Eastward-propagating intraseasonal oscillation represented by Chikira–Sugiyama cumulus parameterization. Part II: Understanding moisture variation under weak temperature gradient balance. *J. Atmos. Sci.*, **71 (2)**, 615–639.

Accepted for publication in *Journal of Climate*. DOI 10.1175/JCLI-D-23-0147.1.

Ciesielski, P. E., R. H. Johnson, P. T. Haertel, and J. Wang, 2003: Corrected toga coare sounding humidity data: Impact on diagnosed properties of convection and climate over the warm pool. *Journal of climate*, **16 (14)**, 2370–2384.

Clark, S. K., Y. Ming, and Á. F. Adames, 2020: Monsoon low pressure system–like variability in an idealized moist model. *Journal of Climate*, **33 (6)**, 2051–2074.

de Szoeke, S. P., 2018: Variations of the moist static energy budget of the tropical indian ocean atmospheric boundary layer. *Journal of the Atmospheric Sciences*, **75 (5)**, 1545–1551, https://doi.org/10.1175/JAS-D-17-0345.1.

Dima, I. M., and J. M. Wallace, 2003: On the seasonality of the hadley cell. *Journal of the atmospheric sciences*, **60 (12)**, 1522–1527.

Edmon Jr, H., B. Hoskins, and M. McIntyre, 1980: Eliassen-palm cross sections for the troposphere. *Journal of Atmospheric Sciences*, **37 (12)**, 2600–2616.

Emanuel, K., 2001: Contribution of tropical cyclones to meridional heat transport by the oceans. *Journal of Geophysical Research: Atmospheres*, **106 (D14)**, 14 771–14 781.

Emanuel, K., 2018: 100 years of progress in tropical cyclone research. *Meteorological Monographs*, **59**, 15–1.

Emanuel, K., 2019: Inferences from simple models of slow, convectively coupled processes. *Journal of the Atmospheric Sciences*, **76 (1)**, 195–208, https://doi.org/10.1175/JAS-D-18-0090.1.

Emanuel, K., A. A. Wing, and E. M. Vincent, 2014: Radiative-convective instability. *J. Adv. Model. Earth Syst.*, **6 (1)**, 75–90.

Feng, T., X.-Q. Yang, J.-Y. Yu, and R. Huang, 2020a: Convective coupling in tropical-depression-type waves. part i: Rainfall characteristics and moisture structure. *Journal of the Atmospheric Sciences*, **77 (10)**, 3407–3422.

Feng, T., X.-Q. Yang, W. Zhou, R. Huang, L. Wu, and D. Yang, 2016: Synoptic-scale waves in sheared background flow over the western north pacific. *Journal of the Atmospheric Sciences*, **73 (11)**, 4583–4603.

Accepted for publication in *Journal of Climate*. DOI 10.1175/JCLI-D-23-0147.1.

Feng, T., J.-Y. Yu, X.-Q. Yang, and R. Huang, 2020b: Convective coupling in tropical-depression-type waves. part ii: Moisture and moist static energy budgets. *Journal of the Atmospheric Sciences*, **77 (10)**, 3423–3440.

Ferreira, R. N., and W. H. Schubert, 1997: Barotropic aspects of itcz breakdown. *Journal of the Atmospheric Sciences*, **54 (2)**, 261–285.

Fuchs, Ž., and D. J. Raymond, 2002: Large-scale modes of a nonrotating atmosphere with water vapor and cloud–radiation feedbacks. *J. Atmos. Sci.*, **59**, 1669–1679.

Gonzalez, A. O., and X. Jiang, 2019: Distinct propagation characteristics of intraseasonal variability over the tropical west pacific. *Journal of Geophysical Research: Atmospheres*, **124 (10)**, 5332–5351, https://doi.org/10.1029/2018JD029884.

Hartmann, D. L., 2015: *Global physical climatology*, Vol. 103. Newnes.

Held, I. M., R. S. Hemler, and V. Ramaswamy, 1993: Radiative-Convective Equilibrium with Explicit Two-Dimensional Moist Convection. *J. Atmos. Sci.*, **50 (23)**, 3909–3927.

Held, I. M., and B. J. Hoskins, 1985: Large-scale eddies and the general circulation of the troposphere. *Advances in geophysics*, Vol. 28, Elsevier, 3–31.

Held, I. M., and A. Y. Hou, 1980: Nonlinear Axially Symmetric Circulations in a Nearly Inviscid Atmosphere. *J. Atmos. Sci.*, **37 (3)**, 515–533.

Herman, M. J., Ž. Fuchs, D. J. Raymond, and P. Bechtold, 2016: Convectively coupled kelvin waves: From linear theory to global models. *J. Atmos. Sci.*, **73 (1)**, 407–428, https://doi.org/10.1175/JAS-D-15-0153.1.

Hersbach, H., and Coauthors, 2020: The era5 global reanalysis. *Quarterly Journal of the Royal Meteorological Society*, **146 (730)**, 1999–2049.

Hohenegger, C., and C. Jakob, 2020: A relationship between itcz organization and subtropical humidity. *Geophysical Research Letters*, **47 (16)**, e2020GL088 515, https://doi.org/https://doi.org/10.1029/2020GL088515.

Holton, J. R., and G. J. Hakim, 2012: *An Introduction to Dynamic Meteorology*. Academic Press.

Accepted for publication in *Journal of Climate*. DOI 10.1175/JCLI-D-23-0147.1.

Huaman, L., E. D. Maloney, C. Schumacher, and G. N. Kiladis, 2021: Easterly waves in the east pacific during the otrec 2019 field campaign. *Journal of the Atmospheric Sciences*, **78 (12)**, 4071–4088.

Inoue, K., Á. F. Adames, and K. Yasunaga, 2020: Vertical Velocity Profiles in Convectively Coupled Equatorial Waves and MJO: New Diagnoses of Vertical Velocity Profiles in the Wavenumber–Frequency Domain. *Journal of the Atmospheric Sciences*, **77 (6)**, 2139–2162, https://doi.org/10.1175/JAS-D-19-0209.1.

Inoue, K., and L. E. Back, 2017: Gross moist stability analysis: Assessment of satellite-based products in the gms plane. *J. Atmos. Sci.*, **74 (6)**, 1819–1837, https://doi.org/10.1175/JAS-D-16-0218.1.

Inoue, K., M. Biasutti, and A. M. Fridlind, 2021: Evidence that horizontal moisture advection regulates the ubiquitous amplification of rainfall variability over tropical oceans. *Journal of the Atmospheric Sciences*, **78 (2)**, 529 – 547, https://doi.org/10.1175/JAS-D-20-0201.1.

Jensen, M. P., and A. D. Del Genio, 2006: Factors limiting convective cloud-top height at the arm nauru island climate research facility. *Journal of climate*, **19 (10)**, 2105–2117.

Jiang, X., and Coauthors, 2020: Fifty years of research on the madden-julian oscillation: Recent progress, challenges, and perspectives. *Journal of Geophysical Research: Atmospheres*, **125 (17)**, e2019JD030 911, https://doi.org/10.1029/2019JD030911.

Kerns, B. W., and S. S. Chen, 2014: Equatorial dry air intrusion and related synoptic variability in mjo initiation during dynamo. *Monthly Weather Review*, **142 (3)**, 1326–1343.

Kiladis, G. N., M. C. Wheeler, P. T. Haertel, K. H. Straub, and P. E. Roundy, 2009: Convectively Coupled Equatorial Waves. *Rev. Geophys.*, 1–42.

Kim, D., M.-S. Ahn, I.-S. Kang, and A. D. Del Genio, 2015: Role of Longwave Cloud–Radiation Feedback in the Simulation of the Madden–Julian Oscillation. *J. Climate*, **28**, 6979–6994.

Kim, J.-E., and C. Zhang, 2021: Core dynamics of the mjo. *Journal of the Atmospheric Sciences*, **78 (1)**, 229 – 248, https://doi.org/10.1175/JAS-D-20-0193.1.

Accepted for publication in *Journal of Climate*. DOI 10.1175/JCLI-D-23-0147.1.

Lau, K.-H., and N.-C. Lau, 1990: Observed Structure and Propagation Characteristics of Tropical Summertime Synoptic Scale Disturbances. *Mon. Wea. Rev.*, **118**, 1888–1913, https://doi.org/10.1175/1520-0493(1990)118⟨1888:OSAPCO⟩2.0.CO;2.

Lau, K.-H., and N.-C. Lau, 1992: The Energetics and Propagation Dynamics of Tropical Summertime Synoptic-Scale Disturbances. *Mon. Wea. Rev.*, **120**, 2523–2539, https://doi.org/10.1175/1520-0493(1992)120⟨2523:TEAPDO⟩2.0.CO;2.

Madden, R., and P. Julian, 1972: Further Evidence of Global-Scale 5-Day Pressure Waves. *J. Atmos. Sci.*, **29 (8)**, 1464–1469.

Maithel, V., 2023: A phase plane based perspective of energetics of large scale tropical convection. Ph.D. thesis, 150 pp.

Maithel, V., and L. Back, 2022: Moisture recharge–discharge cycles: A gross moist stability–based phase angle perspective. *Journal of the Atmospheric Sciences*, **79 (9)**, 2401–2417.

Majda, A. J., and S. N. Stechmann, 2009: The skeleton of tropical intraseasonal oscillations. *Proc. Natl. Acad. Sci. USA*, **106 (21)**, 8417–8422, https://doi.org/10.1073/pnas.0903367106.

Manabe, S., and R. F. Strickler, 1964: Thermal equilibrium of the atmosphere with a convective adjustment. *J. Atmos. Sci.*, **21 (4)**, 361–385.

Mapes, B. E., and P. Zuidema, 1996: Radiative-dynamical consequences of dry tongues in the tropical troposphere. *Journal of Atmospheric Sciences*, **53 (4)**, 620–638.

Matsuno, T., 1966: Quasi-geostrophic motions in the equatorial area. *J. Meteor. Soc. Japan*, **44**, 25–43.

Mayta, V. C., and Á. F. Adames, 2023: Moist Thermodynamics of Convectively Coupled Waves over the Western Hemisphere. *Journal of Climate*, 1–35, https://doi.org/10.1175/JCLI-D-22-0435.1.

Mayta, V. C., Á. F. Adames, and F. Ahmed, 2022: Westward-propagating moisture mode over the tropical western hemisphere. *Geophysical Research Letters*, e2022GL097799.

Accepted for publication in *Journal of Climate*. DOI 10.1175/JCLI-D-23-0147.1.

Mayta, V. C., and Á. F. Adames Corraliza, 2023a: Is the madden-julian oscillation a moisture mode? *Geophysical Research Letters*, **50 (15)**, e2023GL103 002, https://doi.org/https://doi.org/10.1029/2023GL103002.

Mayta, V. C., and Á. F. Adames Corraliza, 2023b: The Stirring Tropics. Part I: The Ubiquity of Moisture Modes and Moisture-Vortex Instability. *Journal of Climate*.

Mooley, D. A., 1973: Some aspects of indian monsoon depressions and the associated rainfall. *Monthly Weather Review*, **101 (3)**, 271–280.

Nakamura, Y., and Y. N. Takayabu, 2022a: Convective couplings with equatorial rossby waves and equatorial kelvin waves. part i: Coupled wave structures. *Journal of the Atmospheric Sciences*, **79 (1)**, 247–262.

Nakamura, Y., and Y. N. Takayabu, 2022b: Convective couplings with equatorial rossby waves and equatorial kelvin waves. part ii: Coupled precipitation characteristics. *Journal of the Atmospheric Sciences*, **79 (11)**, 2919–2933.

Narenpitak, P., C. S. Bretherton, and M. F. Khairoutdinov, 2020: The role of multiscale interaction in tropical cyclogenesis and its predictability in near-global aquaplanet cloud-resolving simulations. *Journal of the Atmospheric Sciences*, **77 (8)**, 2847–2863.

Neelin, J. D., and I. M. Held, 1987: Modeling Tropical Convergence Based on the Moist Static Energy Budget. *Mon. Wea. Rev.*, **115**, 3–12.

Neelin, J. D., and N. Zeng, 2000: A Quasi-Equilibrium Tropical Circulation Model—Formulation*. *J. Atmos. Sci.*, **57 (11)**, 1741–1766.

Núñez Ocasio, K. M., J. L. Evans, and G. S. Young, 2020: A wave-relative framework analysis of aew–mcs interactions leading to tropical cyclogenesis. *Monthly Weather Review*, **148 (11)**, 4657–4671.

Núñez Ocasio, K. M., and R. Rios-Berrios, 2023: African Easterly Wave Evolution and Tropical Cyclogenesis in a Pre-Helene (2006) Hindcast Using the Model for Prediction Across Scales-Atmosphere (MPAS-A). *Journal of Advances in Modeling Earth Systems*, **15 (2)**, e2022MS003 181, https://doi.org/https://doi.org/10.1029/2022MS003181.

Accepted for publication in *Journal of Climate*. DOI 10.1175/JCLI-D-23-0147.1.

Oort, A. H., and J. J. Yienger, 1996: Observed interannual variability in the hadley circulation and its connection to enso. *Journal of Climate*, 2751–2767.

Parsons, D. B., J.-L. Redelsperger, and K. Yoneyama, 2000: The evolution of the tropical western pacific atmosphere-ocean system following the arrival of a dry intrusion. *Quarterly Journal of the Royal Meteorological Society*, **126 (563)**, 517–548.

Peters, M. E., and C. S. Bretherton, 2005: A simplified model of the Walker circulation with an interactive ocean mixed layer and cloud-radiative feedbacks. *J. Climate*, **18 (20)**, 4216–4234.

Peters, M. E., Z. Kuang, and C. C. Walker, 2008: Analysis of atmospheric energy transport in era-40 and implications for simple models of the mean tropical circulation. *Journal of Climate*, **21 (20)**, 5229–5241.

Pierrehumbert, R., 1998: Lateral mixing as a source of subtropical water vapor. *Geophysical research letters*, **25 (2)**, 151–154.

Polvani, L. M., and A. H. Sobel, 2002: The hadley circulation and the weak temperature gradient approximation. *Journal of the atmospheric sciences*, **59 (10)**, 1744–1752.

Popp, M., N. J. Lutsko, and S. Bony, 2020: The relationship between convective clustering and mean tropical climate in aquaplanet simulations. *Journal of advances in modeling earth systems*, **12 (8)**, e2020MS002 070.

Powell, S. W., 2017: Successive mjo propagation in merra-2 reanalysis. *Geophysical Research Letters*, **44 (10)**, 5178–5186, https://doi.org/10.1002/2017GL073399.

Raymond, D., and G. Kilroy, 2019: Control of convection in high-resolution simulations of tropical cyclogenesis. *Journal of Advances in Modeling Earth Systems*, **11 (6)**, 1582–1599.

Raymond, D. J., 2000: Thermodynamic control of tropical rainfall. *Quart. J. Roy. Meteor. Soc.*, **126 (564)**, 889–898, https://doi.org/10.1002/qj.49712656406.

Raymond, D. J., and Ž. Fuchs, 2009: Moisture Modes and the Madden–Julian Oscillation. *J. Climate*, **22**, 3031–3046.

Raymond, D. J., S. L. Sessions, and Ž. Fuchs, 2007: A theory for the spinup of tropical depressions. *Quart. J. Roy. Meteor. Soc.*, **133 (628)**, 1743–1754, https://doi.org/10.1002/qj.125.

Accepted for publication in *Journal of Climate*. DOI 10.1175/JCLI-D-23-0147.1.

Riehl, H., 1954: Tropical meteorology. Tech. rep., McGraw-hill.

Riehl, H., and J. Malkus, 1958: On the heat balance of the equatorial trough zone. *Geophysica*, **6**, 503–538.

Rios-Berrios, R., F. Judt, G. Bryan, B. Medeiros, and W. Wang, 2023: Three-Dimensional Structure of Convectively Coupled Equatorial Waves in Aquaplanet Experiments with Resolved or Parameterized Convection. *Journal of Climate*, 1 – 44, https://doi.org/10.1175/JCLI-D-22-0422.1.

Rios-Berrios, R., B. Medeiros, and G. Bryan, 2020: Mean climate and tropical rainfall variability in aquaplanet simulations using the model for prediction across scales-atmosphere. *Journal of Advances in Modeling Earth Systems*, **12 (10)**, e2020MS002 102.

Rushley, S. S., D. Kim, C. S. Bretherton, and M.-S. Ahn, 2018: Reexamining the Nonlinear Moisture-Precipitation Relationship Over the Tropical Oceans. *Geophys. Res. Lett.*, https://doi.org/10.1002/2017GL076296.

Russell, J. O. H., A. Aiyyer, and J. Dylan White, 2020: African easterly wave dynamics in convection-permitting simulations: Rotational stratiform instability as a conceptual model. *Journal of Advances in Modeling Earth Systems*, **12 (1)**, e2019MS001 706, https://doi.org/10.1029/2019MS001706.

Rydbeck, A. V., and E. D. Maloney, 2014: Energetics of east pacific easterly waves during intraseasonal events. *Journal of Climate*, **27 (20)**, 7603–7621.

Rydbeck, A. V., E. D. Maloney, and G. J. A. Jr., 2017: In situ initiation of east pacific easterly waves in a regional model. *J. Atmos. Sci.*, **74**, 333–351, https://doi.org/10.1175/JAS-D-16-0124.1.

Schiro, K. A., F. Ahmed, S. E. Giangrande, and J. D. Neelin, 2018: Goamazon2014/5 campaign points to deep-inflow approach to deep convection across scales. *Proceedings of the National Academy of Sciences*, **115 (18)**, 4577–4582, https://doi.org/10.1073/pnas.1719842115.

Schneider, E. K., 1977: Axially symmetric steady-state models of the basic state for instability and climate studies. part ii. nonlinear calculations. *Journal of Atmospheric Sciences*, **34 (2)**, 280–296.

Accepted for publication in *Journal of Climate*. DOI 10.1175/JCLI-D-23-0147.1.

Serra, Y. L., G. N. Kiladis, and M. F. Cronin, 2008: Horizontal and Vertical Structure of Easterly Waves in the Pacific ITCZ. *J. Atmos. Sci.*, **65**, 1266–1284, https://doi.org/10.1175/2007JAS2341.1.

Sherwood, S. C., 1996: Maintenance of the free-tropospheric tropical water vapor distribution. part i: Clear regime budget. *Journal of climate*, **9 (11)**, 2903–2918.

Sobel, A., and E. Maloney, 2013: Moisture Modes and the Eastward Propagation of the MJO. *J. Atmos. Sci.*, **70**, 187–192.

Sobel, A., S. Wang, and D. Kim, 2014: Moist static energy budget of the MJO during DYNAMO. *J. Atmos. Sci.*, **71**, 4276–4291.

Sobel, A. H., and C. S. Bretherton, 2000: Modeling Tropical Precipitation in a Single Column. *J. Climate*, **13**, 4378–4392.

Sobel, A. H., and J. D. Neelin, 2006: The boundary layer contribution to intertropical convergence zones in the quasi-equilibrium tropical circulation model framework. *Theoretical and Computational Fluid Dynamics*, **20**, 323–350.

Sobel, A. H., J. Nilsson, and L. M. Polvani, 2001: The Weak Temperature Gradient Approximation and Balanced Tropical Moisture Waves. *J. Atmos. Sci.*, **58**, 3650–3665.

Stachnik, J. P., and C. Schumacher, 2011: A comparison of the hadley circulation in modern reanalyses. *Journal of Geophysical Research: Atmospheres*, **116 (D22)**.

Stoll, P. J., R. G. Graversen, and G. Messori, 2023: The global atmospheric energy transport analysed by a wavelength-based scale separation. *Weather and Climate Dynamics*, **4 (1)**, 1–17.

Sugiyama, M., 2009: The Moisture Mode in the Quasi-Equilibrium Tropical Circulation Model. Part I: Analysis Based on the Weak Temperature Gradient Approximation. *J. Atmos. Sci.*, **66**, 1507–1523.

Tam, C.-Y., and T. Li, 2006: The origin and dispersion characteristics of the observed tropical summertime synoptic-scale waves over the western pacific. *Monthly weather review*, **134 (6)**, 1630–1646.

Accepted for publication in *Journal of Climate*. DOI 10.1175/JCLI-D-23-0147.1.

Tang, B. H., R. Rios-Berrios, J. J. Alland, J. D. Berman, and K. L. Corbosiero, 2016: Sensitivity of axisymmetric tropical cyclone spinup time to dry air aloft. *Journal of the Atmospheric Sciences*, **73 (11)**, 4269–4287.

Tang, B. H., and Coauthors, 2020: Recent advances in research on tropical cyclogenesis. *Tropical Cyclone Research and Review*, **9 (2)**, 87–105.

Thorncroft, C., and B. Hoskins, 1994: An idealized study of african easterly waves. i: A linear view. *Quarterly Journal of the Royal Meteorological Society*, **120 (518)**, 953–982.

Torres, V. M., C. D. Thorncroft, and N. M. Hall, 2021: Genesis of easterly waves over the tropical eastern pacific and the intra-americas sea. *Journal of the Atmospheric Sciences*, **78 (10)**, 3263–3279.

Trenberth, K. E., and D. P. Stepaniak, 2003: Covariability of components of poleward atmospheric energy transports on seasonal and interannual timescales. *Journal of climate*, **16 (22)**, 3691–3705.

Vallis, G. K., 2017: *Atmospheric and oceanic fluid dynamics*, Vol. 2. Cambridge University Press.

Vargas Martes, R. M., Á. F. Adames Corraliza, and V. C. Mayta, 2023: The role of water vapor and temperature in the thermodynamics of tropical northeast pacific and african easterly waves. *Journal of the Atmospheric Sciences*.

Windmiller, J. M., and G. C. Craig, 2019: Universality in the spatial evolution of self-aggregation of tropical convection. *Journal of the Atmospheric Sciences*, **76 (6)**, 1677–1696.

Wing, A. A., and K. A. Emanuel, 2014: Physical mechanisms controlling self-aggregation of convection in idealized numerical modeling simulations. *J. Adv. Model. Earth Syst.*, **6 (1)**, 59–74.

Wolding, B., J. Dias, G. Kiladis, F. Ahmed, S. W. Powell, E. Maloney, and M. Branson, 2020: Interactions between moisture and tropical convection. part i: The coevolution of moisture and convection. *Journal of the Atmospheric Sciences*, **77 (5)**, 1783–1799, https://doi.org/10.1175/JAS-D-19-0225.1.

Accepted for publication in *Journal of Climate*. DOI 10.1175/JCLI-D-23-0147.1.

Wolding, B., S. W. Powell, F. Ahmed, J. Dias, M. Gehne, G. Kiladis, and J. D. Neelin, 2022: Tropical thermodynamic–convection coupling in observations and reanalyses. *Journal of the Atmospheric Sciences*, **79 (7)**, 1781–1803.

Wolding, B. O., E. D. Maloney, and M. Branson, 2016: Vertically resolved weak temperature gradient analysis of the Madden-Julian Oscillation in SP-CESM. *J. Adv. Model. Earth Syst.*, https://doi.org/10.1002/2016MS000724.

Yanai, M., S. Esbensen, and J. Chu, 1973: Determination of bulk properties of tropical cloud clusters from large-scale heat and moisture budgets. *J. Atmos. Sci.*, **30**, 611–627, https://doi.org/10.1175/1520-0469(1973)030⟨0611:DOBPOT⟩2.0.CO;2.

Yasunaga, K., S. Yokoi, K. Inoue, and B. E. Mapes, 2019: Space–time spectral analysis of the moist static energy budget equation. *J. Climate*, **32 (2)**, 501–529, https://doi.org/10.1175/JCLI-D-18-0334.1.

Yoshida, R., Y. Miyamoto, H. Tomita, and Y. Kajikawa, 2017: The effect of water vapor on tropical cyclone genesis: A numerical experiment of a non-developing disturbance observed in palau2010. *Journal of the Meteorological Society of Japan. Ser. II*, **95 (1)**, 35–47.

Yu, J.-Y., C. Chou, and J. D. Neelin, 1998: Estimating the gross moist stability of the tropical atmosphere. *J. Atmos. Sci.*, **55 (8)**, 1354–1372, https://doi.org/10.1175/1520-0469(1998)055⟨1354:ETGMSO⟩2.0.CO;2.

Yu, J.-Y., and J. D. Neelin, 1994: Modes of Tropical Variability under Convective Adjustment and the Madden–Julian Oscillation. Part II: Numerical Results. *Journal of the Atmospheric Sciences*, **51 (13)**, 1895–1914, https://doi.org/10.1175/1520-0469(1994)051⟨1895:MOTVUC⟩2.0.CO;2.

Zhang, C., Á. F. Adames, B. Khouider, B. Wang, and D. Yang, 2020: Four theories of the madden-julian oscillation. *Reviews of Geophysics*, **58 (3)**, e2019RG000 685, https://doi.org/10.1029/2019RG000685.

Accepted for publication in *Journal of Climate*. DOI 10.1175/JCLI-D-23-0147.1.